

---

# Exploring the Synergy of Quantitative Factors and Newsflow Representations from Large Language Models for Stock Return Prediction

---

**Tian Guo** **Emmanuel Hauptmann**  
Systematic Equities Team, RAM Active Investments  
Geneva, Switzerland  
`{tig, eh}@ram-ai.com`

## Abstract

In quantitative investing, return prediction supports various tasks, including stock selection, portfolio optimization, and risk management. Quantitative factors, such as valuation, quality, and growth, capture various characteristics of stocks. Unstructured financial data, like news and transcripts, has attracted growing attention, driven by recent advances in large language models (LLMs). This paper examines effective methods for leveraging multimodal factors and newsflow in return prediction and stock selection. First, we introduce a fusion learning framework to learn a unified representation from factors and newsflow representations generated by an LLM. Within this framework, we compare three representative methods: representation combination, representation summation, and attentive representations. Next, building on empirical observations from fusion learning, we explore the mixture model that adaptively combines predictions made by single modalities and their fusion. To mitigate the training instability observed in the mixture model, we introduce a decoupled training approach with theoretical insights. Finally, our experiments on real investment universes reveal: (1) Within fusion learning, the representation combination method, despite its relatively low architectural complexity, generally outperforms the other fusion methods. This suggests that, in noisy financial environments, effective fusion can be achieved by employing simple model architectures that operate across the set of modality-specific representations. (2) The mixture model achieves comparable or superior performance relative to fusion learning, depending on investment universes. Its enhanced adaptability may be particularly beneficial in universes where the relative predictive relevance of news and factors is likely more variable. (3) Fine-tuning the LLM during the training of multimodal prediction models does not consistently benefit performance; its impact varies across investment universes, potentially reflecting differences in market efficiency and characteristics.

## 1 Introduction

Quantitative investing involves using numerical features, also referred to as quantitative factors, derived from diverse data sources (e.g., prices, economic indicators, and analyst estimates), to select stocks and construct portfolios [26, 2]. Traditional quantitative factors, e.g., value, momentum, and growth, have demonstrated predictive power for market movements in numerous studies. Recently, the incorporation of textual data like financial news, earnings call transcripts, and annual reports has gained significant traction, driven by advances in large language models (LLMs) [52, 57, 46, 53].

This paper focuses on predicting stock returns using multimodal quantitative factors and financial newsflow, as illustrated in Fig. 1. Accurate return forecasting is essential for subsequent tasks like stock selection and portfolio optimization [28, 17]. Quantitative factors, grounded in financial the-

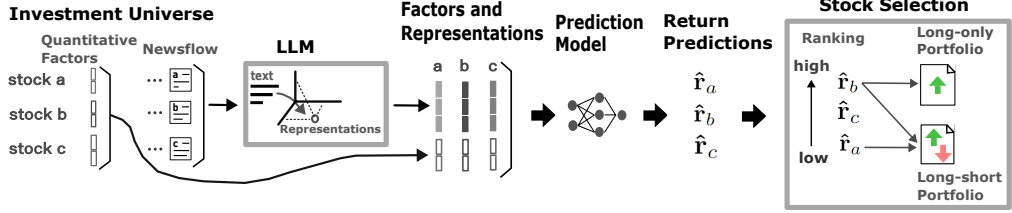


Figure 1: Workflow using quantitative factors and newsflow for return prediction and stock selection.

ory, capture fundamental aspects of stocks, while financial news provides timely information about company events and actions. These two modalities offer complementary perspectives, making their integration promising for prediction tasks [54, 81, 74].

While quantitative factors and financial newsflow have each been studied separately in existing works [15, 24, 30, 53], combining them poses several challenges. First, the two modalities differ fundamentally in structure: quantitative factors are structured and numeric, while newsflow is unstructured and textual. Second, their predictive relevance, that is, the degree to which each modality relates to stock returns, can vary. News, in particular, is context-dependent and may often be less relevant or provide little incremental information relative to factors that already capture (or price in) various aspects of stocks [33, 66, 24, 28]. Even after filtering out irrelevant news, which remains a non-trivial task in practice, the relative predictive relevance of news versus factors can still fluctuate depending on data characteristics and market conditions.

**Contributions.** This paper investigates effective model designs and training methods for using quantitative factors and newsflow in return prediction and stock selection. Our contributions are:

(1) We formulate the problem of return prediction and stock selection using multimodal factors and newsflow. We introduce a multimodal fusion learning framework to learn unified representations by combining factors with newsflow representations generated by an LLM. In this framework, we compare three methods of distinct architectural complexity: representation combination, representation summation, and attentive representation.

(2) Motivated by empirical comparison in fusion learning, we explore the mixture model that adaptively weights the predictions made by single modalities and their fusion. This enables information integration at both the representation and prediction levels. We observe that conventional training of such mixture models often leads to instability and performance degradation. To mitigate this issue, we provide theoretical insights into the cause and introduce a decoupled training method.

(3) We conduct experiments on real data across multiple investment universes. We build long-only and long-short portfolios using return predictions and evaluate their backtest performance. In addition, we compare results obtained without and with LLM fine-tuning during the training of prediction models. These experiments yield several insights into effective multimodal modeling of factors and news for stock return prediction, which are summarized in the Conclusion section.

## 2 Related Work

**Multimodal Learning for Finance.** Integrating multimodal data has gained increasing attention in finance [5, 8, 78]. [8, 34] developed multimodal financial LLMs for various analytical tasks. For prediction tasks, social media and event data were used with numerical features to capture sentiment and event-driven price dynamics [70, 73, 68]. Some works developed graph and attention-based methods to fuse multimodal data for predicting volatilities and earnings [3, 41]. This paper presents a comparative study of different multimodal fusion methods for return prediction and stock selection.

**LLMs in Quantitative Investment.** Previous works used word-level embedding techniques for modeling stock and forex movements [44, 33, 16]. Recent advances in LLMs have significantly improved contextual understanding and can generate powerful numeric representations of text for prediction tasks [62, 30, 59]. [6, 45, 36] fine-tuned pre-trained LLMs for financial sentiment extraction. [46, 65, 40, 63] employed prompt-based methods to harness the reasoning capabilities of LLMs over financial data. [39] utilized chain-of-thought prompts [69] to analyze financial state-

ments. [53] trained LLMs using temporally split datasets to mitigate look-ahead bias. [43] used retrieval-augmented data to improve financial analysis. [20] developed the sentiment and return prediction models with LLM-generated text representations of news.

In this paper, we use the newsflow representations generated by an LLM in fusion learning and mixture modeling. Meanwhile, we compare the performance with and without fine-tuning the LLM during the training of our multimodal prediction models [32].

**Mixture Models for Financial Predictions.** Mixture models enable adaptive learning to combine multiple specialized components [75, 58, 5]. [61] trained mixtures of stock return prediction components using price-based features, but did not indicate the specialization of each mixture component. [23] developed a mixture of LLMs, i.e., a separate LLM for each type of financial data and an additional LLM for aggregating the predictions, without the need for a model training process. [56] combined several pre-trained expert LLMs through filtering for online time-series prediction tasks.

The mixture model in this paper involves prediction components that correspond to single modalities and their fusion. Moreover, we identify instability in the conventional training of this mixture model, analyze its causes, and introduce a specialized training method with theoretical insights.

### 3 Factors and Newsflow for Return Prediction and Stock Selection

#### 3.1 Problem Statement

We consider an investment universe consisting of a set of stocks denoted by  $\mathcal{U} = \{s\}_{s=1}^S$ , where each  $s$  represents a stock index. The prediction target is the  $\ell$ -step forward return of stock  $s$  at time  $t$ , denoted by  $r_{s,t+\ell} \in \mathbb{R}$ . For a target  $r_{s,t+\ell}$ , we define the corresponding vector of quantitative factors of stock  $s$  at timestamp  $t$  as  $\mathbf{x}_{s,t,f} \in \mathbb{R}^{d_f}$ .

Meanwhile, we use stock-specific news, referring to news reporting events related to a company (e.g., earnings releases, management changes, product launches). A news item published at time  $i$  for stock  $s$  is denoted by  $\mathbf{N}_{s,i}$ . To predict  $r_{s,t+\ell}$ , we collect the news in a look-back window before time  $t$ , forming the newsflow  $\{\mathbf{N}_{s,i}\}_{i \in \mathcal{T}_{s,<t}}$  where  $\mathcal{T}_{s,<t}$  represents the set of relevant timesteps.

Following prior works [30, 62, 7], we adopt a simple approach without trainable parameters to obtain the newsflow representation  $\mathbf{x}_{s,t,n} \in \mathbb{R}^{d_n}$ : feeding  $\{\mathbf{N}_{s,i}\}_{i \in \mathcal{T}_{s,<t}}$  into an LLM and aggregating the resulting token representations into one vector  $\mathbf{x}_{s,t,n}$ . The LLM can be fine-tuned by backpropagating through  $\mathbf{x}_{s,t,n}$  when training the prediction model, as illustrated in Fig. 2.

The training data is formed by collecting instances across stocks and timestamps, denoted as  $\mathcal{D} := \{(\mathbf{x}_{s,t,f}, \mathbf{x}_{s,t,n}, r_{s,t+\ell})\}_{s \in \mathcal{U}, t \in \mathcal{T}}$ , where  $\mathcal{T}$  represents the timestamps in the training period. For simplicity, we omit the indices  $s$  and  $t$  in the remainder of the paper and denote a generic instance sample as  $\{\mathbf{x}_f, \mathbf{x}_n, r\} \sim \mathcal{D}$ .

At test time, we evaluate an important application of return predictions: selecting stocks into Long-Only and Long-Short portfolios and backtesting their performance [28, 15], as illustrated in Fig. 1.

Long-Only Portfolios include stocks with the expectation of the highest forward return. In practice, it is built by ranking the stocks based on return predictions and selecting the top- $K$  stocks.  $K$  is usually chosen according to the decile or quantile of the universe, e.g., 10% of the number of stocks.

Long-Short Portfolios include stocks with the highest and lowest return expectations. The stocks with the lowest returns are expected to experience a price drop, and the portfolio can profit by selling them at the current price and repurchasing them at a lower price in the future. It is built by including the top- $K$  and bottom- $K$  stocks based on return predictions.

#### 3.2 Methodologies

In this section, we explore two categories of approaches as illustrated in Fig. 2. First, from a multimodal learning perspective, it is essential to obtain a unified representation that effectively integrates information from different modalities [81, 74]. Accordingly, we present a representation-level fusion learning framework that combines factors and newsflow representations into a unified representation for return prediction.

However, while factors grounded in financial theories tend to offer relatively stable predictive power [28], news data is inherently noisy and its predictive relevance depends on its content and the information it provides beyond factors [66]. Although fusion learning can leverage attention mechanisms to weight modalities, it ultimately predicts based on unified representations, thereby entangling factor and news information. This lack of explicit separation of different predictive relevance can undermine performance, as illustrated in Fig. 3.

Subsequently, we explore the mixture model that adaptively combines predictions separately generated from factors and unified representations.

### 3.2.1 Fusion Learning over Factors and Newsflow Representations

Our fusion learning framework comprises two functions: a representation fusion function and a prediction function, as formulated in Eq. 1:

$$\hat{r} = g(\mathbf{x}_u) \quad \mathbf{x}_u = z(\mathbf{x}_f, \mathbf{x}_n) \quad (1)$$

$$\min_{\theta_u} \mathbb{E}_{\{\mathbf{x}_f, \mathbf{x}_n, r\} \sim \mathcal{D}} [(r - \hat{r})^2] \quad (2)$$

, where  $z(\cdot, \cdot)$  denotes the fusion function that integrates the factors and newsflow representations into a unified representation  $\mathbf{x}_u$ .  $g(\cdot)$  is the prediction function mapping  $\mathbf{x}_u$  to the predicted return  $\hat{r}$ . The trainable parameters  $\theta_u$ , including those in both the fusion and prediction functions, are optimized via stochastic gradient descent-based optimization to minimize the expected squared error between the predicted return  $\hat{r}$  and the true value  $r$  as Eq. 2. Within this framework, different fusion strategies can be instantiated by specifying the form of  $z(\cdot, \cdot)$ .

Next, we present three representative methods that span a range of architectural complexities, from simple dense layer-based to attention-based fusion (with implementation details in the Appendix).

**Representation Combination.** By treating each dimension of the newsflow representation as a feature alongside the numerical factors, combinations of all these features form a unified representation [48]. A straightforward approach is to concatenate the two and pass through a dense layer that learns arbitrary nonlinear weighted combinations of input features [19, 79], as Eq. 3:

$$z(\mathbf{x}_f, \mathbf{x}_n) = h(\mathbf{x}_f \oplus \mathbf{x}_n) \quad (3)$$

, where  $h(\cdot)$  represents a dense layer, and  $\oplus$  denotes the concatenation operation.

**Representation Summation.** By assuming a shared representation space, the Representation Summation method projects each modality into a vector of equal dimensionality and then sums these projected representations [38, 67], thereby encouraging modality alignment, as shown in Eq. 4:

$$z(\mathbf{x}_f, \mathbf{x}_n) = h_f(\mathbf{x}_f) + h_n(\mathbf{x}_n) \quad (4)$$

, where  $h_f(\cdot)$  and  $h_n(\cdot)$  represent the projection functions that map respective inputs to the representation vectors and can be implemented, for instance, using dense layers.

**Attentive Representation.** Extending the Representation Summation method, we introduce modality-wise weights to adapt the fusion behavior across instances [50, 41], as defined in Eq. 5:

$$z(\mathbf{x}_f, \mathbf{x}_n) = a_f h_f(\mathbf{x}_f) + a_n h_n(\mathbf{x}_n) \quad (5)$$

$$[a_f, a_n] = \text{softmax}(w(\mathbf{x}_f, \mathbf{x}_n)) \quad (6)$$

, where  $a_f$  and  $a_n$  are scalar weights, satisfying  $0 \leq a_f, a_n \leq 1$ .  $h_f(\cdot)$  and  $h_n(\cdot)$  are as defined in Eq. 4. Then, in Eq. 6,  $w(\cdot, \cdot)$  is a logits function producing two unnormalized scores.

**Empirical Observations Motivating the Mixture Model.** We briefly discuss the illustrative comparison in Fig. 3 and leave the full results and analysis to the experiment and appendix sections. In Fig. 3, there are four blocks, each with different methods indicated on the x-axis.

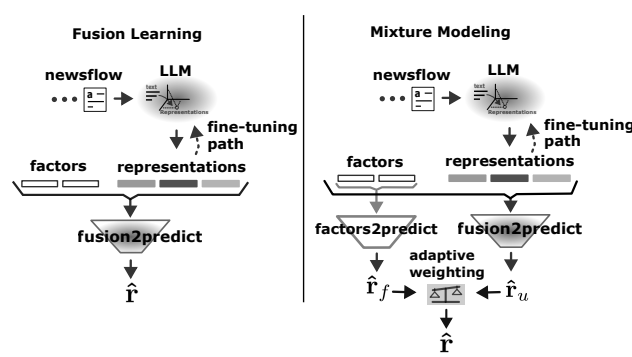


Figure 2: Illustration of fusion learning and mixture model.

In the leftmost block of Fig. 3, *Factors Alone* and *News Alone* are single-modal methods (with details in the experiment and Appendix sections). In the Fusion Learning block, *Combination*, *Summation*, and *Attention* correspond to the three methods presented above. The Mixture Conventional and Mixture Decoupled blocks denote mixture models trained under different schemes, as discussed in the next subsection.

In the Fusion Learning block of Fig. 3, *Combination*, i.e., the representation combination method, achieves superior performance compared with *News Alone* in the Single Modal block. This suggests that fusion learning can generate predictive representations, with the effectiveness depending on specific methods. In this example, the relatively simple *Combination* method outperforms complex alternatives.

However, a comparison with the *Factors Alone* method in Fig. 3 reveals a limitation of fusion learning. While the *Combination* method improves the long-only portfolio, it underperforms in the long-short portfolio, indicating its weaker predictive performance for low-return stocks, compared to *Factors Alone*. This behavior may arise when newsflow is less relevant or offers little incremental information for certain instances or market regimes; in such cases, fusion learning dilutes information from factors and reduces performance, as illustrated here for low-return stocks. More generally, this dilution effect may manifest across stocks and time, as the relative informativeness of factors and news evolves.

### 3.2.2 Mixture Modeling over Factors-based and Fusion-based Predictions

Based on the above analysis of Fig. 3, it is desirable to include factors in a separate prediction component and to adaptively leverage the factors-based and fusion-based predictions when they excel under different conditions. To this end, we present the mixture model that consists of two prediction components (with implementation details in the Appendix):

$$\hat{r} = \sum_{i \in \{f, u\}} p_\phi(I = i | \mathbf{x}_f, \mathbf{x}_n) \cdot g_{\theta_i}(\mathbf{x}_i) \quad (7)$$

$$[p_\phi(I = f | \mathbf{x}_f, \mathbf{x}_n), p_\phi(I = u | \mathbf{x}_f, \mathbf{x}_n)] = \text{softmax}(\ell_\phi(\mathbf{x}_f, \mathbf{x}_n)) \quad (8)$$

In Eq. 7, let  $i \in \{f, u\}$  index the prediction components.  $i = f$  refers to the factors-based prediction component  $g_{\theta_f}(\mathbf{x}_f)$ , and  $i = u$  refers to the fusion-based prediction component  $g_{\theta_u}(\mathbf{x}_u)$ . The factors-based prediction function  $g_{\theta_f}(\mathbf{x}_f)$  is implemented as a dense network parameterized by  $\theta_f$ . Motivated by the competitive performance of the representation combination method in experiments, the fusion-based component  $g_{\theta_u}(\cdot)$  with input  $\mathbf{x}_u$  follows the formulation in Eq. 1 and Eq. 3.

The prediction weights are defined as a probability distribution  $p_\phi(I | \mathbf{x}_f, \mathbf{x}_n)$  over the component index  $I \in \{f, u\}$ , which facilitates the formulation of the subsequent decoupled training. In Eq. 8, let  $\ell_\phi : \mathbb{R}^{d_f} \times \mathbb{R}^{d_n} \rightarrow \mathbb{R}^2$  be a logits function parameterized by  $\phi$ , which takes the factors  $\mathbf{x}_f \in \mathbb{R}^{d_f}$  and the newsflow representation  $\mathbf{x}_n \in \mathbb{R}^{d_n}$  and outputs a vector of two unnormalized scores (logits) corresponding to the two predictions.

**Limitations of Conventional Training.** The conventional training of the mixture model minimizes the squared errors over training data as:

$$\min_{\theta_f, \theta_u, \phi} \mathbb{E}_{\{\mathbf{x}_f, \mathbf{x}_n, r\} \sim \mathcal{D}} \left[ \left[ r - \sum_{i \in \{f, u\}} p_\phi(I = i | \mathbf{x}_f, \mathbf{x}_n) \cdot g_{\theta_i}(\mathbf{x}_i) \right]^2 \right] \quad (9)$$

However, empirically, we observe that this conventional training often leads to unstable convergence of individual components and degraded performance [29]. For instance, in Fig. 4a, under conventional training, the training error curves of the mixture model’s two prediction components exhibit

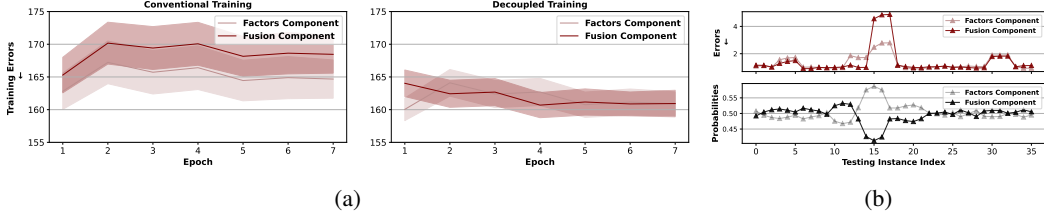


Figure 4: (a) Training error curves of the mixture model’s prediction components by different training methods. (b) Illustration of the alignment between each component’s prediction errors (top panel) and mixture probabilities (bottom panel) learned via the distribution matching in decoupled training. Note that the x-axis represents test samples ordered arbitrarily (not a time series).

slow and unstable convergence. In the Mixture Conventional block of Fig. 3, *Factors* and *Fusion* correspond to the return predictions of the respective components within the mixture model, while *Overall* represents the combined mixture predictions. Compared with *Factors Alone* and *Combination* under standalone training, the *Factors* and *Fusion* components show performance degradation. Consequently, the mixture model fails to achieve satisfactory overall performance, as shown in the *Overall* result.

Fundamentally, as presented in Proposition 1 (with proof and extended discussion in the Appendix), the conventional training is affected by entangled gradient variance.

**Proposition 1 (Entangled Gradient Variance).** *Consider stochastic gradient descent with instances sampled as  $\{\mathbf{x}_f, \mathbf{x}_n, r\} \sim \mathcal{D}$ . Let  $\hat{r}$  denote the model’s prediction. Let  $i$  index a prediction component in the mixture model, and define the gradient signal for component  $i$  as  $\zeta_i := (r - \hat{r}) \cdot \nabla_{\theta_i} g_{\theta_i}(\mathbf{x}_i)$ , where  $\theta_i$  are the parameters of the  $i$ -th prediction component. Define  $p_i := p_\phi(I = i | \mathbf{x}_f, \mathbf{x}_n)$ . Under the conventional training objective given in Eq. 9, the variance of the stochastic gradient  $\delta_i$  used to update  $\theta_i$  is:*

$$\text{Var}(\delta_i) = 4\mathbb{E}^2[p_i] \text{Var}(\zeta_i) + 4\mathbb{E}[\|\zeta_i\|^2] \text{Var}(p_i) \quad (10)$$

By contrast, under the standalone training of component  $i$ , the gradient variance is:

$$\text{Var}(\delta_i) = 4 \text{Var}(\zeta_i) \quad (11)$$

From standard results in stochastic optimization [12, 10], the convergence behavior is closely tied to the variance of stochastic gradients on training data. The convergence rate is generally bounded by  $\mathcal{O}(\text{Var}(\delta)/\sqrt{k})$ .  $\text{Var}(\delta)$  denotes the variance of stochastic gradient  $\delta$ , and  $k$  is the iteration step.

As shown in Eq. 10, the unstable convergence of the mixture model’s components is related to the gradient variance arising from the variances of  $\zeta_i$  and  $p_i$  with additional entanglement through their respective expectations. This entanglement implies that even if individual variances are moderate, their interaction can amplify the total variance. In particular,  $\mathbb{E}[\|\zeta_i\|^2]$  can be large due to the number of parameters in prediction components implemented by dense networks. Meanwhile, since all prediction components influence the residual  $r - \hat{r}$  in the mixture model, an inaccurate component can inflate the residual, thereby increasing the variance. By contrast, the standalone training of a prediction component, such as the fusion learning in Sec. 3.2.1, has no such entanglement in Eq. 11.

**Decoupled Training.** Given the above observations and analysis, we propose the decoupled training method (with theoretical insights in the Appendix).

The key idea is to train each prediction component independently to realize its predictive capacity, while learning the probability distribution based on the actual relative performance of each component. Concretely, the decoupled training minimizes the loss function comprising two parts:

$$\min_{\theta_f, \theta_u, \phi} \mathbb{E}_{\{\mathbf{x}_f, \mathbf{x}_n, r\} \sim \mathcal{D}} \left[ \underbrace{L(\theta_f, \theta_u; \{\mathbf{x}_f, \mathbf{x}_n, r\})}_{\text{Independent Training}} + \underbrace{L(\phi; \{\mathbf{x}_f, \mathbf{x}_n, r\}, \hat{\theta}_f, \hat{\theta}_u)}_{\text{Distribution Matching}} \right] \quad (12)$$

$$L(\theta_f, \theta_u; \{\mathbf{x}_f, \mathbf{x}_n, r\}) := \sum_{i \in \{f, u\}} [r - g_{\theta_i}(\mathbf{x}_i)]^2 \quad (13)$$

$$L(\phi; \{\mathbf{x}_f, \mathbf{x}_n, r\}, \hat{\theta}_f, \hat{\theta}_u) := \text{KL} \left[ p_\phi(I | \mathbf{x}_f, \mathbf{x}_n) \parallel p_{\hat{\theta}_f, \hat{\theta}_u}(I | \mathbf{x}_f, \mathbf{x}_n, r) \right] \quad (14)$$

The Independent Training term  $L(\theta_f, \theta_u; \cdot)$  involves solely the parameters  $\theta_f$  and  $\theta_u$  for training prediction components. It is realized by minimizing the squared error of each component in Eq. 13.

The Distribution Matching term  $L(\phi; \cdot)$  aligns the mixture probability  $p_\phi(I | \mathbf{x}_f, \mathbf{x}_n)$  with a target distribution  $p_{\hat{\theta}_f, \hat{\theta}_u}(I | \mathbf{x}_f, \mathbf{x}_n, r)$  that reflects the actual relative prediction performance of each component on each data instance. Here,  $\hat{\theta}_f$  and  $\hat{\theta}_u$  denote the given parameter values of the prediction components. In Eq. 14, minimizing the Kullback–Leibler (KL) divergence, with respect to  $\phi$ , encourages  $p_\phi(I | \mathbf{x}_f, \mathbf{x}_n)$  to allocate probabilities in accordance with the relative prediction performance indicated in  $p_{\hat{\theta}_f, \hat{\theta}_u}(I | \mathbf{x}_f, \mathbf{x}_n, r)$ . The KL divergence between discrete distributions is analytically tractable and fits into stochastic gradient descent-based optimization [9].

Specifically, the target distribution  $p_{\hat{\theta}_f, \hat{\theta}_u}(I | \mathbf{x}_f, \mathbf{x}_n, r)$  is defined in Eq. 15:

$$[p_{\hat{\theta}_f, \hat{\theta}_u}(I = f | \cdot), p_{\hat{\theta}_f, \hat{\theta}_u}(I = u | \cdot)] = \text{softmax} \left( - (r - g_{\hat{\theta}_f}(\mathbf{x}_f))^2 / \tau, - (r - g_{\hat{\theta}_u}(\mathbf{x}_u))^2 / \tau \right) \quad (15)$$

In Eq. 15, the softmax function takes as input the prediction errors of the two components, negatively scaled by the temperature parameter  $\tau$ . The output probabilities  $p_{\hat{\theta}_f, \hat{\theta}_u}(I | \cdot)$  reflect the relative prediction performance by assigning higher probabilities to components with lower prediction errors. For brevity, we omit  $(\mathbf{x}_f, \mathbf{x}_u, r)$  in the conditioning notation of  $p_{\hat{\theta}_f, \hat{\theta}_u}(I | \cdot)$ . The terms  $g_{\hat{\theta}_f}(\mathbf{x}_f)$  and  $g_{\hat{\theta}_u}(\mathbf{x}_u)$  in Eq. 15 represent the respective predictions of the two components.

During training, we adopt a simple estimate for  $\hat{\theta}_f$  and  $\hat{\theta}_u$ , i.e., using the most recent values. For instance, at step  $k$ ,  $\hat{\theta}_f$  is set to the value of  $\theta_f$  from step  $k - 1$ . Thus,  $p_{\hat{\theta}_f, \hat{\theta}_u}(I | \cdot)$  reflects the latest learned predictive performance of each component and becomes increasingly reliable as training progresses. Exploring alternative estimation methods is left for future work.

At test time, when  $r$  is not available and  $p_{\hat{\theta}_f, \hat{\theta}_u}(I | \cdot)$  cannot be computed,  $p_\phi(I | \mathbf{x}_f, \mathbf{x}_n)$  serves to infer the relative performance of each component and then to combine the predictions as Eq. 7. For instance, Fig. 4b illustrates the alignment learned through distribution matching: in general, components with higher prediction errors receive lower probabilities, and vice versa.

Compared with conventional training, in Fig. 4a, under decoupled training, the training error curves of the two prediction components present relatively stable convergence and lower errors. Accordingly, in the Mixture Decoupled block of Fig. 3, the *Factors* and *Fusion* components achieve performance comparable to *Factors Alone* and *Combination*, respectively. The overall performance of the mixture model is notably improved relative to conventional training.

## 4 Experiments

In this section, we briefly present the experiment setup and discuss primarily the results from one investment universe. The full experiment details and results for all universes are in the Appendix.

**Data.** We have three investment universe datasets covering the North American (NA), European (EU), and Emerging (EM) markets. Each entry in these datasets consists of the date, the stock identifier, a vector of quantitative factors, and the stock’s monthly forward return relative to that date. We use company-level financial news data provided by a commercial data vendor. In the Appendix, Table 3 and 4 list the main categories of factors and news included in our dataset, while Table 5 presents the statistics of training, validation, and testing data.

**Baselines.** For a fair comparison, we employ the encoder-only LLM, DeBERTa [31], across our fusion learning methods, mixture models, and all LLM-based baselines. Universe refers to a portfolio that equally weights all stocks in the investment universe. Factors Alone represents a dense neural network solely on quantitative factors [17]. Note that for a fair comparison, in the mixture model, the factors-based prediction component adopts the same model structure as this baseline. News Alone utilizes only news by employing a prediction layer on the news representations generated by an LLM [30]. FININ develops a factors-based attention to weight newsflow representations before jointly passing both through a prediction layer [66].

**Setup.** For training, we use the one-month forward return as the target variable, as the subsequent backtest focuses on monthly rebalanced portfolios. After training, the model is evaluated on the

Table 1: Portfolio and prediction performance of the North American Universe. The best and second-best results are highlighted with dark gray and light gray boxes, respectively.

	Long-only Portfolios		Long-short Portfolios		Prediction Metrics	
	Ann. Return % ( $\uparrow$ )	Sharpe Ratio ( $\uparrow$ )	Ann. Return % ( $\uparrow$ )	Sharpe Ratio ( $\uparrow$ )	MAPE ( $\downarrow$ )	IC ( $\uparrow$ )
Universe	12.37	0.84	—	—	—	—
Factors Alone	22.31	0.81	22.34	1.26	1.352	0.018
News Alone	20.96	1.03	1.08	0.18	1.092	-0.0
FININ	23.12	0.83	18.16	1.16	1.467	0.019
Fusion Combination	32.43	1.0	28.41	1.64	1.402	0.031
Fusion Summation	20.42	0.76	16.13	1.03	1.465	0.017
Fusion Attention	21.73	0.73	19.59	0.87	1.302	-0.005
Mixture Conventional	23.27	0.75	29.32	1.42	1.539	0.016
Mixture Decoupled	28.21	0.92	33.77	1.78	1.319	0.027

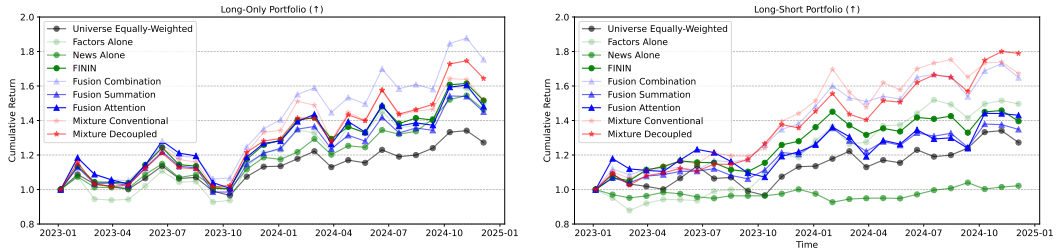


Figure 5: Performance Charts of the North American Universe.

testing period without retraining in a rolling manner. The testing period covers 2023 and 2024 for mitigating potential memorization bias in LLM [53, 42, 47] (with explanations in the Appendix).

For fine-tuning, we applied Low-Rank Adaptation (LoRA) to all layers of DeBERTa [32]. Other techniques, including gradient checkpointing, mixed precision training, and DeepSpeed, are used to reduce GPU memory [22, 55].

During backtesting, the long-only portfolio consists of stocks in the top (9th) decile of predicted returns, while the long-short portfolio holds stocks in both the top (9th) and bottom (0th) deciles [30, 15]. Both portfolios are equally weighted and rebalanced monthly.

**Metrics.** We use annualized returns and Sharpe ratios for evaluating portfolio performance, and Mean Absolute Percentage Error (MAPE) and the Information Coefficient (IC) as prediction metrics [24]. Results are reported both without and with LLM fine-tuning. Additionally, we present the bar charts of decile returns to illustrate the sources of portfolio performance.

**Results.** Table 1 reports the portfolio and prediction performance, while Fig. 5 visualizes the cumulative returns of corresponding portfolios. *Fusion Combination*, *Fusion Summation*, and *Fusion Attention* refer to the three methods in fusion learning. *Mixture Conventional* and *Mixture Decoupled* represent the mixture model trained under the conventional and decoupled schemes.

**Portfolio Performance.** In Table 1, within the fusion learning group, *Fusion Combination* achieves superior performance in both long-only and long-short portfolios. Compared with the baselines, FININ performs reasonably well but still lags *Fusion Combination*. The weaker portfolio performance of other fusion methods may stem from their tendency to compress heterogeneous modalities into a shared representation space, potentially obscuring or destroying complementary information [14]. The precise cause necessitates further investigation in future work. Overall, these results suggest that preserving the structure of each modality and learning across the set of modality-specific representations can yield effective predictive representations.

Meanwhile, in Table 1, *Mixture Decoupled* demonstrates competitive performance and robustness across portfolios, indicating that decoupled training helps unlock the potential of the mixture model. Specifically, in long-only portfolios, *Mixture Decoupled* trails the top-performing *Fusion Combination*. In long-short portfolios, *Mixture Decoupled* becomes the best-performing method and improves upon its long-only results, indicating that the short part of the portfolio contributes positively. By contrast, *Fusion Combination*, the top performer in the long-only portfolio, delivers a lower return in the long-short setting, reflecting an underperforming short part.

**Gap between Prediction Errors and Stock Selection Efficacy.** The MAPE results in Table 1 demonstrate that a low MAPE does not guarantee a high-performing portfolio, highlighting the difference between a model’s predictive error and its practical effectiveness in stock selection [21, 35]. For instance, consider the *Fusion Attention* method, which has a relatively low MAPE; yet it delivers a weaker portfolio performance. MAPE assesses average prediction errors across test data and is largely insensitive to the relative ordering of predicted returns, which is crucial for stock selection. Moreover, MAPE is symmetric: it penalizes over- and under-predictions of the same magnitude equally. For instance, in stock selection, a small under-prediction may push a truly high-return stock out of the top decile, while a comparable over-prediction may incorrectly include a mid-return stock into the top decile. Thus, a model with a low MAPE may still fail to identify the high-return or low-return stocks, leading to suboptimal portfolio performance.

**IC as a Relevant Indicator.** The IC results in Table 1 provide an indicator more relevant to portfolio performance [77, 24]. Although these IC values may appear small, in quantitative finance, a small positive IC can indicate meaningful predictive power and lead to effective stock selection on a large universe of stocks. Among the methods, *Fusion Combination* achieves the highest IC, followed by *Mixture Decoupled*, consistent with their strong performance in long-only and long-short portfolios.

**Decile-Level Comparison.** Fig. 6, a bar chart of decile returns, provides a granular view of the investment performance across the deciles of predicted returns [30] and illustrates the sources of the portfolio performance in Table 1. Specifically, a decile return, or the average return per predicted decile, is obtained by sorting stocks based on their predicted returns and then grouping them into ten deciles, labeled 0 through 9. The 0th decile contains the stocks with the lowest predicted returns, while the 9th decile includes those with the highest predicted returns. For each decile, we then compute the average return of the stocks within that group.

Ideally, the decile returns should exhibit a strong spread: very negative (or low) returns for the 0th decile (the short leg) and very high returns for the 9th decile (the long leg). For the long leg, *Fusion Combination* and *Mixture Decoupled* achieve high returns in the 9th decile, consistent with their long-only portfolio performance in Table 1. The distinction lies in the short leg of the portfolio: only *Mixture Decoupled* delivers the desired negative return in the 0th decile, whereas *Fusion Combination* still produces a positive return. This explains why *Mixture Decoupled* outperforms *Fusion Combination* in the long-short portfolio: the short leg contributes more effectively, enhancing the overall long-short spread.

**Inconsistent Impact of Fine-Tuning the LLM.** Table 2 reports the portfolio and prediction performance without and with enabling LLM fine-tuning during the training of prediction models in the NA universe. Only the methods using an LLM are included in Table 2, and the results without fine-tuning are from Table 1. Corresponding results for the EM and EU universes are in Tables 9 and 11 in the Appendix.

The results in Table 2, Table 9, and Table 11 demonstrate that enabling fine-tuning during training has a universe-dependent impact [11]. The NA universe is a highly efficient market where public information, like news, is often quickly priced in and absorbed into factors [1]. In this context, fine-tuning the LLM in multimodal models might cause it to overemphasize the already-priced or noisy news information, thereby marginally affecting or even weakening performance. In contrast, EM and EU universes tend to be more heterogeneous and less efficient [13, 27]. In these markets, news may contain more nuanced and unpriced information, making fine-tuning act as a specialization

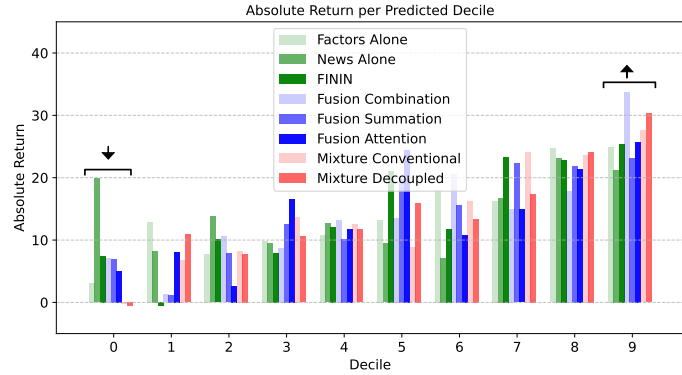


Figure 6: Decile Returns of the North American Universe. The arrows on the 0th and 9th deciles indicate the desired direction of values. A lower return is preferred for the 0th decile, as it represents the short leg of a long-short portfolio.

Table 2: Portfolio and prediction performance without and with enabling LLM fine-tuning during training for the North American Universe. The best and second-best results within each group (without fine-tuning and with fine-tuning) are highlighted with dark gray █ and light gray █ boxes.

		Long-only Portfolios		Long-short Portfolios		Prediction Metrics	
		Ann. Return % (↑)	Sharpe Ratio (↑)	Ann. Return % (↑)	Sharpe Ratio (↑)	MAPE (↓)	IC (↑)
w/o Fine-tuning	News Alone	20.96	<span style="background-color: #808080; border: 1px solid black;">1.03</span>	1.08	0.18	<span style="background-color: #808080; border: 1px solid black;">1.092</span>	-0.0
	FININ	23.12	0.83	18.16	1.16	1.467	0.019
	Fusion Combination	<span style="background-color: #808080; border: 1px solid black;">32.43</span>	<span style="background-color: #808080; border: 1px solid black;">1.0</span>	28.41	<span style="background-color: #808080; border: 1px solid black;">1.64</span>	1.402	<span style="background-color: #808080; border: 1px solid black;">0.031</span>
	Fusion Summation	20.42	0.76	16.13	1.03	1.465	0.017
	Fusion Attention	21.73	0.73	19.59	0.87	<span style="background-color: #808080; border: 1px solid black;">1.302</span>	-0.005
	Mixture Conventional	23.27	0.75	<span style="background-color: #808080; border: 1px solid black;">29.32</span>	1.42	1.539	0.016
	Mixture Decoupled	28.21	0.92	<span style="background-color: #808080; border: 1px solid black;">33.77</span>	<span style="background-color: #808080; border: 1px solid black;">1.78</span>	1.319	<span style="background-color: #808080; border: 1px solid black;">0.027</span>
w/ Fine-tuning	News Alone	27.98	<span style="background-color: #808080; border: 1px solid black;">1.33</span>	14.23	1.52	<span style="background-color: #808080; border: 1px solid black;">1.118</span>	0.018
	FININ	22.09	0.81	19.65	1.24	1.468	0.02
	Fusion Combination	<span style="background-color: #808080; border: 1px solid black;">28.61</span>	<span style="background-color: #808080; border: 1px solid black;">0.95</span>	26.82	<span style="background-color: #808080; border: 1px solid black;">1.63</span>	1.379	<span style="background-color: #808080; border: 1px solid black;">0.032</span>
	Fusion Summation	20.69	0.77	18.31	1.12	1.477	0.017
	Fusion Attention	17.12	0.63	13.55	0.7	<span style="background-color: #808080; border: 1px solid black;">1.298</span>	-0.004
	Mixture Conventional	26.57	0.85	<span style="background-color: #808080; border: 1px solid black;">32.23</span>	1.43	1.326	0.017
	Mixture Decoupled	27.15	0.91	30.66	<span style="background-color: #808080; border: 1px solid black;">1.79</span>	1.336	<span style="background-color: #808080; border: 1px solid black;">0.028</span>

process with the potential for improvement. These findings highlight the need for future research into adaptive fine-tuning strategies tailored to the different characteristics of investment universes.

Specifically, in Table 2, for most of the multimodal methods (Fusion and Mixture groups), fine-tuning appears to have a detrimental effect. Conversely, the single-modal *News Alone* method, which relies solely on the LLM without factors, shows a notable improvement. With fine-tuning enabled, *Fusion Combination* remains the top performer in the long-only portfolio, although its performance declines. Within the Mixture group, *Mixture Decoupled* experiences a more pronounced performance drop, although its Sharpe ratios remain strong relative to *Mixture Conventional*. This may be because, in the *Mixture Decoupled*, the fusion-based component is obtained through the independent training term in Eq. 12 and is therefore more susceptible to the adverse effects of fine-tuning, consistent with the observations in the Fusion group.

## 5 Conclusion

This paper explores effective model design and training schemes for utilizing multimodal factors and newsflow for return prediction and stock selection. First, we introduce a representation-level fusion learning framework, realized through three representative methods. Second, given the limitation of fusion learning observed in empirical comparison, we propose a mixture model that adaptively combines predictions made by single modalities and their fusion. To mitigate the training instability of mixture models, we introduce a decoupled training scheme with theoretical insights.

**Findings.** Experiments across different investment universes reveal the following findings:

- (i) Fusion learning achieves competitive performance and outperforms the news-alone method. This indicates that integrating multimodal factors and news can produce predictive representations; however, the effectiveness depends on specific methods. For the data examined in this paper, the representation combination method, despite its relatively simple architecture, outperforms complex alternatives. This suggests that, in noisy financial environments, effective fusion can be achieved by using simple model architectures that operate across the full set of modality-specific representations.
- (ii) The mixture model achieves performance that is comparable to or better than fusion learning, with notable gains in certain universes. Its enhanced adaptability may be advantageous in universes where the relative predictive power of news and factors tends to be more variable. Moreover, the performance improvement from the decoupled training highlights the importance of specialized training schemes for models involving entangled components.
- (iii) Contrary to the intuition that fine-tuning an LLM would consistently enhance performance, our results reveal an inconsistent impact of fine-tuning during the training of our multimodal models. This appears to depend on market efficiency and characteristics. In highly efficient markets like the NA universe, fine-tuning tends to overfit certain news information that is likely already priced in by factors, thereby disrupting the complementary fusion and degrading overall performance. In contrast, in heterogeneous and less efficient markets, such as the EM and EU universes, fine-tuning yields performance improvements.

## 6 Future Work

Open problems remain for future research, for instance:

- Financial text often contains less relevant information that can lead models to capture spurious relations. Given the instruction-following capabilities of LLMs [72], it is promising to explore their use for improving data quality, for instance, by filtering, cleaning, or summarizing news content. Such preprocessing can help enhance downstream prediction tasks and potentially improve the risk profile of portfolios constructed based on return predictions.
- Several recent LLMs for text embedding have demonstrated strong performance [60, 80]. It would be valuable to compare the proposed methods in this paper with these new LLMs.
- While the mixture model adaptively combines predictions, further work could exploit diverse contextual data, such as market regimes and macroeconomic environments [4], to inform and refine the probability weighting and distribution matching.
- It would also be worthwhile to evaluate how the proposed methods perform when additional data sources are incorporated, such as earnings call transcripts, market time series, and so on [41, 79].
- The inconsistent impact of fine-tuning the LLM during the training of multimodal prediction models highlights the need for future research into adaptive fine-tuning strategies tailored to the characteristics of different investment universes [37].

## References

- [1] Luiz GA Alves, Higor YD Sigaki, Matjaž Perc, and Haroldo V Ribeiro. Collective dynamics of stock market efficiency. *Scientific reports*, 10(1):21992, 2020.
- [2] Andrew Ang. *Asset management: A systematic approach to factor investing*. Oxford University Press, 2014.
- [3] Gary Ang and Ee-Peng Lim. Guided attention multimodal multitask financial forecasting with inter-company relationships and global and local news. In *Proceedings of the 60th Annual Meeting of the Association for Computational Linguistics (Volume 1: Long Papers)*, pages 6313–6326, 2022.
- [4] Nino Antulov-Fantulin, Alvaro Cauderan, and Petter N Kolm. A dynamic regime-switching model using gated recurrent straight-through units. *Journal of Financial Data Science*, 6(4), 2024.
- [5] Nino Antulov-Fantulin, Tian Guo, and Fabrizio Lillo. Temporal mixture ensemble models for probabilistic forecasting of intraday cryptocurrency volume. *Decisions in Economics and Finance*, 44(2):905–940, 2021.
- [6] Dogu Araci. Finbert: Financial sentiment analysis with pre-trained language models. *arXiv preprint arXiv:1908.10063*, 2019.
- [7] Parishad BehnamGhader, Vaibhav Adlakha, Marius Mosbach, Dzmitry Bahdanau, Nicolas Chapados, and Siva Reddy. Llm2vec: Large language models are secretly powerful text encoders. *arXiv preprint arXiv:2404.05961*, 2024.
- [8] Gagan Bhatia, Hasan Cavusoglu, Muhammad Abdul-Mageed, et al. Fintral: A family of gpt-4 level multimodal financial large language models. In *Findings of the Association for Computational Linguistics ACL 2024*, pages 13064–13087, 2024.
- [9] David M Blei, Alp Kucukelbir, and Jon D McAuliffe. Variational inference: A review for statisticians. *Journal of the American statistical Association*, 112(518):859–877, 2017.
- [10] Léon Bottou, Frank E Curtis, and Jorge Nocedal. Optimization methods for large-scale machine learning. *SIAM review*, 60(2):223–311, 2018.
- [11] Meni Brief, Oded Ovadia, Gil Shenderovitz, Noga Ben Yoash, Rachel Lemberg, and Eitam Sheerit. Mixing it up: The cocktail effect of multi-task fine-tuning on llm performance—a case study in finance. *arXiv preprint arXiv:2410.01109*, 2024.
- [12] Sébastien Bubeck et al. Convex optimization: Algorithms and complexity. *Foundations and Trends® in Machine Learning*, 8(3-4):231–357, 2015.

- [13] Charles W Calomiris and Harry Mamaysky. How news and its context drive risk and returns around the world. *Journal of Financial Economics*, 133(2):299–336, 2019.
- [14] Abhra Chaudhuri, Anjan Dutta, Tu Bui, and Serban Georgescu. A closer look at multi-modal representation collapse. In *Forty-second International Conference on Machine Learning*. PMLR, 2022.
- [15] Lakshay Chauhan, John Alberg, and Zachary Lipton. Uncertainty-aware lookahead factor models for quantitative investing. In *International Conference on Machine Learning*, pages 1489–1499. PMLR, 2020.
- [16] Deli Chen, Keiko Harimoto, Ruihan Bao, Qi Su, Xu Sun, et al. Group, extract and aggregate: Summarizing a large amount of finance news for forex movement prediction. *arXiv preprint arXiv:1910.05032*, 2019.
- [17] Luyang Chen, Markus Pelger, and Jason Zhu. Deep learning in asset pricing. *Management Science*, 70(2):714–750, 2024.
- [18] Qinkai Chen. Stock movement prediction with financial news using contextualized embedding from bert. *arXiv preprint arXiv:2107.08721*, 2021.
- [19] Yen-Chun Chen, Linjie Li, Licheng Yu, Ahmed El Kholy, Faisal Ahmed, Zhe Gan, Yu Cheng, and Jingjing Liu. Uniter: Universal image-text representation learning. In *European conference on computer vision*, pages 104–120. Springer, 2020.
- [20] Yifei Chen, Bryan T Kelly, and Dacheng Xiu. Expected returns and large language models. *Available at SSRN 4416687*, 2022.
- [21] Jean Dessimain. Machine learning models predicting returns: Why most popular performance metrics are misleading and proposal for an efficient metric. *Expert Systems with Applications*, 199:116970, 2022.
- [22] Ning Ding, Yujia Qin, Guang Yang, Fuchao Wei, Zonghan Yang, Yusheng Su, Shengding Hu, Yulin Chen, Chi-Min Chan, Weize Chen, et al. Parameter-efficient fine-tuning of large-scale pre-trained language models. *Nature Machine Intelligence*, 5(3):220–235, 2023.
- [23] Qianggang Ding, Haochen Shi, Jiadong Guo, and Bang Liu. Tradexpert: Revolutionizing trading with mixture of expert llms. *arXiv preprint arXiv:2411.00782*, 2024.
- [24] Yitong Duan, Lei Wang, Qizhong Zhang, and Jian Li. Factorvae: A probabilistic dynamic factor model based on variational autoencoder for predicting cross-sectional stock returns. In *Proceedings of the AAAI Conference on Artificial Intelligence*, volume 36, pages 4468–4476, 2022.
- [25] Joseph Engelberg, Asaf Manela, William Mullins, and Luka Vulicevic. Entity neutering. *Available at SSRN*, 2025.
- [26] Eugene F Fama and Kenneth R French. Multifactor explanations of asset pricing anomalies. *The journal of finance*, 51(1):55–84, 1996.
- [27] Jiali Fang and Ben Jacobsen. Cross-country determinants of market efficiency: a technical analysis perspective. *Journal of Banking & Finance*, 169:107297, 2024.
- [28] Shihao Gu, Bryan Kelly, and Dacheng Xiu. Empirical asset pricing via machine learning. *The Review of Financial Studies*, 33(5):2223–2273, 2020.
- [29] Tian Guo. Learning mixture structure on multi-source time series for probabilistic forecasting. In *A causal view on dynamical systems, NeurIPS 2022 workshop*.
- [30] Tian Guo and Emmanuel Hauptmann. Fine-tuning large language models for stock return prediction using newsflow. In *Proceedings of the 2024 Conference on Empirical Methods in Natural Language Processing: Industry Track*, pages 1028–1045, 2024.
- [31] Pengcheng He, Jianfeng Gao, and Weizhu Chen. Debertav3: Improving deberta using electra-style pre-training with gradient-disentangled embedding sharing. *arXiv preprint arXiv:2111.09543*, 2021.
- [32] Edward J Hu, Yelong Shen, Phillip Wallis, Zeyuan Allen-Zhu, Yuanzhi Li, Shean Wang, Lu Wang, and Weizhu Chen. Lora: Low-rank adaptation of large language models. *arXiv preprint arXiv:2106.09685*, 2021.

[33] Ziniu Hu, Weiqing Liu, Jiang Bian, Xuanzhe Liu, and Tie-Yan Liu. Listening to chaotic whispers: A deep learning framework for news-oriented stock trend prediction. In *Proceedings of the eleventh ACM international conference on web search and data mining*, pages 261–269, 2018.

[34] Jimin Huang, Mengxi Xiao, Dong Li, Zihao Jiang, Yuzhe Yang, Yifei Zhang, Lingfei Qian, Yan Wang, Xueqing Peng, Yang Ren, et al. Open-finllms: Open multimodal large language models for financial applications. *arXiv preprint arXiv:2408.11878*, 2024.

[35] Ondřej Hubáček and Gustav Šír. Beating the market with a bad predictive model. *International journal of forecasting*, 39(2):691–719, 2023.

[36] Giorgos Iacovides, Thanos Konstantinidis, Mingxue Xu, and Danilo Mandic. Finllama: Llm-based financial sentiment analysis for algorithmic trading. In *Proceedings of the 5th ACM International Conference on AI in Finance*, pages 134–141, 2024.

[37] Zixuan Ke, Yifei Ming, Xuan-Phi Nguyen, Caiming Xiong, and Shafiq Joty. Demystifying domain-adaptive post-training for financial llms. *arXiv preprint arXiv:2501.04961*, 2025.

[38] Douwe Kiela, Edouard Grave, Armand Joulin, and Tomas Mikolov. Efficient large-scale multi-modal classification. In *Proceedings of the AAAI conference on artificial intelligence*, volume 32, 2018.

[39] Alex Kim, Maximilian Muhn, and Valeri V Nikolaev. Financial statement analysis with large language models. *Chicago Booth Research Paper Forthcoming, Fama-Miller Working Paper*, 2024.

[40] Kelvin JL Koa, Yunshan Ma, Ritchie Ng, and Tat-Seng Chua. Learning to generate explainable stock predictions using self-reflective large language models. In *Proceedings of the ACM on Web Conference 2024*, pages 4304–4315, 2024.

[41] Ross Koval, Nicholas Andrews, and Xifeng Yan. Financial forecasting from textual and tabular time series. In *Findings of the Association for Computational Linguistics: EMNLP 2024*, pages 8289–8300, 2024.

[42] Bradford Levy. Caution ahead: Numerical reasoning and look-ahead bias in ai models. Available at SSRN 5082861, 2024.

[43] Xiang Li, Zhenyu Li, Chen Shi, Yong Xu, Qing Du, Mingkui Tan, and Jun Huang. Alphafin: Benchmarking financial analysis with retrieval-augmented stock-chain framework. In *Proceedings of the 2024 Joint International Conference on Computational Linguistics, Language Resources and Evaluation (LREC-COLING 2024)*, pages 773–783, 2024.

[44] Qikai Liu, Xiang Cheng, Sen Su, and Shuguang Zhu. Hierarchical complementary attention network for predicting stock price movements with news. In *Proceedings of the 27th ACM International Conference on Information and Knowledge Management*, pages 1603–1606, 2018.

[45] Zhuang Liu, Degen Huang, Kaiyu Huang, Zhuang Li, and Jun Zhao. Finbert: A pre-trained financial language representation model for financial text mining. In *Proceedings of the twenty-ninth international conference on international joint conferences on artificial intelligence*, pages 4513–4519, 2021.

[46] Alejandro Lopez-Lira and Yuehua Tang. Can chatgpt forecast stock price movements? return predictability and large language models. *arXiv preprint arXiv:2304.07619*, 2023.

[47] Alejandro Lopez-Lira, Yuehua Tang, and Mingyin Zhu. The memorization problem: Can we trust llms’ economic forecasts? *arXiv preprint arXiv:2504.14765*, 2025.

[48] Seungwhan Moon, Andrea Madotto, Zhaojiang Lin, Tushar Nagarajan, Matt Smith, Shashank Jain, Chun-Fu Yeh, Prakash Murugesan, Peyman Heidari, Yue Liu, et al. Anymal: An efficient and scalable any-modality augmented language model. In *Proceedings of the 2024 Conference on Empirical Methods in Natural Language Processing: Industry Track*, pages 1314–1332, 2024.

[49] Iftikhar Muhammad and Marco Rospocher. On assessing the performance of llms for target-level sentiment analysis in financial news headlines. *Algorithms*, 18(1):46, 2025.

[50] Arsha Nagrani, Shan Yang, Anurag Arnab, Aren Jansen, Cordelia Schmid, and Chen Sun. Attention bottlenecks for multimodal fusion. *Advances in neural information processing systems*, 34:14200–14213, 2021.

[51] Adam Paszke, Sam Gross, Francisco Massa, Adam Lerer, James Bradbury, Gregory Chanan, Trevor Killeen, Zeming Lin, Natalia Gimelshein, Luca Antiga, et al. Pytorch: An imperative style, high-performance deep learning library. *Advances in neural information processing systems*, 32, 2019.

[52] Yu Qin and Yi Yang. What you say and how you say it matters: Predicting financial risk using verbal and vocal cues. In *57th Annual Meeting of the Association for Computational Linguistics (ACL 2019)*, page 390, 2019.

[53] Eghbal Rahimikia and Felix Drinkall. Re(visiting) large language models in finance. *Available at SSRN*, 2024.

[54] Divya Ramachandram and Yi Han Tay. Deep multimodal learning: A survey. *ACM Computing Surveys (CSUR)*, 52(6):1–71, 2019.

[55] Jeff Rasley, Samyam Rajbhandari, Olatunji Ruwase, and Yuxiong He. Deepspeed: System optimizations enable training deep learning models with over 100 billion parameters. In *Proceedings of the 26th ACM SIGKDD International Conference on Knowledge Discovery & Data Mining*, pages 3505–3506, 2020.

[56] Raeid Saqr, Anastasis Kratsios, Florian Krach, Yannick Limmer, Blanka Horvath, and Frank Rudzicz. Filtered not mixed: Filtering-based online gating for mixture of large language models. In *The Thirteenth International Conference on Learning Representations*, 2025.

[57] Ramit Sawhney, Shivam Agarwal, Arnav Wadhwa, and Rajiv Shah. Deep attentive learning for stock movement prediction from social media text and company correlations. In *Proceedings of the 2020 Conference on Empirical Methods in Natural Language Processing (EMNLP)*, pages 8415–8426, 2020.

[58] Yuge Shi, Brooks Paige, Philip Torr, et al. Variational mixture-of-experts autoencoders for multi-modal deep generative models. *Advances in neural information processing systems*, 32, 2019.

[59] Xingyou Song, Oscar Li, Chansoo Lee, Bangding Yang, Daiyi Peng, Sagi Perel, and Yutian Chen. Omnipred: Language models as universal regressors. *Transactions on Machine Learning Research*, 2024.

[60] Saba Sturua, Isabelle Mohr, Mohammad Kalim Akram, Michael Günther, Bo Wang, Markus Krimmel, Feng Wang, Georgios Mastrapas, Andreas Koukounas, Nan Wang, et al. jina-embeddings-v3: Multilingual embeddings with task lora. *arXiv preprint arXiv:2409.10173*, 2024.

[61] Shuo Sun, Xinrun Wang, Wanqi Xue, Xiaoxuan Lou, and Bo An. Mastering stock markets with efficient mixture of diversified trading experts. In *Proceedings of the 29th ACM SIGKDD Conference on Knowledge Discovery and Data Mining*, pages 2109–2119, 2023.

[62] Eric Tang, Bangding Yang, and Xingyou Song. Understanding llm embeddings for regression. *arXiv preprint arXiv:2411.14708*, 2024.

[63] Hanshuang Tong, Jun Li, Ning Wu, Ming Gong, Dongmei Zhang, and Qi Zhang. Ploutos: Towards interpretable stock movement prediction with financial large language model. *arXiv preprint arXiv:2403.00782*, 2024.

[64] Ashish Vaswani, Noam Shazeer, Niki Parmar, Jakob Uszkoreit, Llion Jones, Aidan N Gomez, Łukasz Kaiser, and Illia Polosukhin. Attention is all you need. In *Advances in neural information processing systems*, pages 5998–6008, 2017.

[65] Meiyun Wang, Kiyoshi Izumi, and Hiroki Sakaji. Llmfactor: Extracting profitable factors through prompts for explainable stock movement prediction. *arXiv preprint arXiv:2406.10811*, 2024.

[66] Mengyu Wang, Shay B Cohen, and Tiejun Ma. Modeling news interactions and influence for financial market prediction. In *Findings of the Association for Computational Linguistics: EMNLP 2024*, pages 3302–3314, 2024.

[67] Peng Wang, An Yang, Rui Men, Junyang Lin, Shuai Bai, Zhikang Li, Jianxin Ma, Chang Zhou, Jingren Zhou, and Hongxia Yang. Ofa: Unifying architectures, tasks, and modalities through a simple sequence-to-sequence learning framework. In *International conference on machine learning*, pages 23318–23340. PMLR, 2022.

[68] Yaowei Wang, Qing Li, Zhexue Huang, and Junjie Li. Ean: Event attention network for stock price trend prediction based on sentimental embedding. In *Proceedings of the 10th ACM Conference on Web Science*, pages 311–320, 2019.

[69] Jason Wei, Xuezhi Wang, Dale Schuurmans, Maarten Bosma, Fei Xia, Ed Chi, Quoc V Le, Denny Zhou, et al. Chain-of-thought prompting elicits reasoning in large language models. *Advances in neural information processing systems*, 35:24824–24837, 2022.

[70] Bin Weng, Lin Lu, Xing Wang, Fadel M Megahed, and Waldyn Martinez. Predicting short-term stock prices using ensemble methods and online data sources. *Expert Systems with Applications*, 112:258–273, 2018.

[71] Thomas Wolf, Lysandre Debut, Victor Sanh, Julien Chaumond, Clement Delangue, Anthony Moi, Pierrick Cistac, Tim Rault, Rémi Louf, Morgan Funtowicz, et al. Huggingface’s transformers: State-of-the-art natural language processing. *arXiv preprint arXiv:1910.03771*, 2019.

[72] Qianqian Xie, Weiguang Han, Xiao Zhang, Yanzhao Lai, Min Peng, Alejandro Lopez-Lira, and Jimin Huang. Pixiu: a large language model, instruction data and evaluation benchmark for finance. In *Proceedings of the 37th International Conference on Neural Information Processing Systems*, pages 33469–33484, 2023.

[73] Yumo Xu and Shay B Cohen. Stock movement prediction from tweets and historical prices. In *Proceedings of the 56th Annual Meeting of the Association for Computational Linguistics (Volume 1: Long Papers)*, pages 1970–1979, 2018.

[74] Yuan Yuan, Zhaojian Li, and Bin Zhao. A survey of multimodal learning: Methods, applications, and future. *ACM Computing Surveys*, 57(7):1–34, 2025.

[75] Seniha Esen Yuksel, Joseph N Wilson, and Paul D Gader. Twenty years of mixture of experts. *IEEE transactions on neural networks and learning systems*, 23(8):1177–1193, 2012.

[76] Cheng Zhang, Judith Bütepage, Hedvig Kjellström, and Stephan Mandt. Advances in variational inference. *IEEE transactions on pattern analysis and machine intelligence*, 41(8):2008–2026, 2018.

[77] Feng Zhang, Ruite Guo, and Honggao Cao. Information coefficient as a performance measure of stock selection models. *arXiv preprint arXiv:2010.08601*, 2020.

[78] Wentao Zhang, Lingxuan Zhao, Haochong Xia, Shuo Sun, Jiaze Sun, Molei Qin, Xinyi Li, Yuqing Zhao, Yilei Zhao, Xinyu Cai, et al. A multimodal foundation agent for financial trading: Tool-augmented, diversified, and generalist. In *Proceedings of the 30th ACM SIGKDD conference on knowledge discovery and data mining*, pages 4314–4325, 2024.

[79] Yang Zhang, Wenbo Yang, Jun Wang, Qiang Ma, and Jie Xiong. Camef: Causal-augmented multi-modality event-driven financial forecasting by integrating time series patterns and salient macroeconomic announcements. In *Proceedings of the 31st ACM SIGKDD Conference on Knowledge Discovery and Data Mining V. 2*, pages 3867–3878, 2025.

[80] Yanzhao Zhang, Mingxin Li, Dingkun Long, Xin Zhang, Huan Lin, Baosong Yang, Pengjun Xie, An Yang, Dayiheng Liu, Junyang Lin, Fei Huang, and Jingren Zhou. Qwen3 embedding: Advancing text embedding and reranking through foundation models. *arXiv preprint arXiv:2506.05176*, 2025.

[81] Jinan Zou, Qingying Zhao, Yang Jiao, Haiyao Cao, Yanxi Liu, Qingsen Yan, Ehsan Abbasnejad, Lingqiao Liu, and Javen Qinfeng Shi. Stock market prediction via deep learning techniques: A survey. *arXiv preprint arXiv:2212.12717*, 2022.

# Appendix

## Table of Contents

<b>A Proof and Discussion</b>	<b>16</b>
<b>B Theoretical Insights of Decoupled Training</b>	<b>18</b>
<b>C Experiment Details and Full Results</b>	<b>19</b>
C.1 Datasets . . . . .	19
C.2 Baselines . . . . .	20
C.3 Implementations . . . . .	20
C.4 Training and Evaluation Setup . . . . .	21
C.5 Metrics . . . . .	21
C.6 Results of the North American Universe . . . . .	22
C.7 Results of the Emerging Markets Universe . . . . .	24
C.8 Results of the European Universe . . . . .	26

## A Proof and Discussion

**Proposition 1. (Entangled Gradient Variance)** Consider stochastic gradient descent with data instances sampled as  $\{\mathbf{x}_f, \mathbf{x}_n, r\} \sim \mathcal{D}$ . Let  $\hat{r}$  denote the model's prediction. Let  $i$  index a prediction component in the mixture model, and define the gradient signal for component  $i$  as  $\zeta_i := (r - \hat{r}) \cdot \nabla_{\theta_i} g_{\theta_i}(\mathbf{x}_i)$ , where  $\theta_i$  are the parameters of the  $i$ -th prediction component. Define  $p_i := p_{\phi}(I = i | \mathbf{x}_f, \mathbf{x}_n)$ . Under the conventional training objective given in Eq. 9, the variance of the stochastic gradient  $\delta_i$  used to update  $\theta_i$  is:

$$\text{Var}(\delta_i) = 4\mathbb{E}^2[p_i] \text{Var}(\zeta_i) + 4\mathbb{E}[\|\zeta_i\|^2] \text{Var}(p_i)$$

By contrast, under the standalone training of component  $i$ , the gradient variance is:

$$\text{Var}(\delta_i) = 4 \text{Var}(\zeta_i)$$

*Proof.* When training the mixture model using stochastic gradient descent-based optimization, given one training instance  $\{\mathbf{x}_f, \mathbf{x}_n, r\}$ , the prediction is  $\hat{r} = \sum_{i \in \{f, c\}} p_{\phi}(I = i | \mathbf{x}_f, \mathbf{x}_n) \cdot g_{\theta_i}(\mathbf{x}_i)$ , and the joint squared loss is  $[r - \hat{r}]^2$ .

The stochastic gradient of the squared loss with respect to the prediction component  $i$  is

$$\delta_i = -2p_i(r - \hat{r}) \nabla_{\theta_i} g_{\theta_i}(\mathbf{x}_i) \quad (16)$$

where  $p_i := p_{\phi}(I = i | \mathbf{x}_f, \mathbf{x}_n)$ .

Let  $\zeta_i$  be the gradient multiplied by the prediction residual, i.e.,  $\zeta_i := (r - \hat{r}) \nabla_{\theta_i} \hat{r} = (r - \hat{r}) \nabla_{\theta_i} g_{\theta_i}(\mathbf{x}_i)$ , and thus the gradient of the prediction component's parameters  $\theta_i$  takes the form:

$$\delta_i = -2p_i \cdot \zeta_i \quad (17)$$

Assume  $\zeta_i$  and  $p_i$  are independent. Based on the identity for the variance of the product of two independent variables  $\text{Var}[XY] = \text{Var}[X]\text{Var}[Y] + \text{Var}[X]\mathbb{E}^2[Y] + \text{Var}[Y]\mathbb{E}^2[X]$ , the variance of the stochastic gradient  $\delta_i$  over the training data distribution is:

$$\text{Var}(\delta_i) = 4 \left[ \mathbb{E}^2[p_i] \text{Var}(\zeta_i) + \|\mathbb{E}[\zeta_i]\|^2 \text{Var}(p_i) + \text{Var}(p_i) \text{Var}(\zeta_i) \right] \quad (18)$$

$$= 4[\mathbb{E}^2[p_i] + \text{Var}(p_i)] \text{Var}(\zeta_i) + 4\|\mathbb{E}[\zeta_i]\|^2 \text{Var}(p_i) \quad (19)$$

$$= 4\mathbb{E}^2[p_i] \text{Var}(\zeta_i) + 4\mathbb{E}[\|\zeta_i\|^2] \text{Var}(p_i) \quad (20)$$

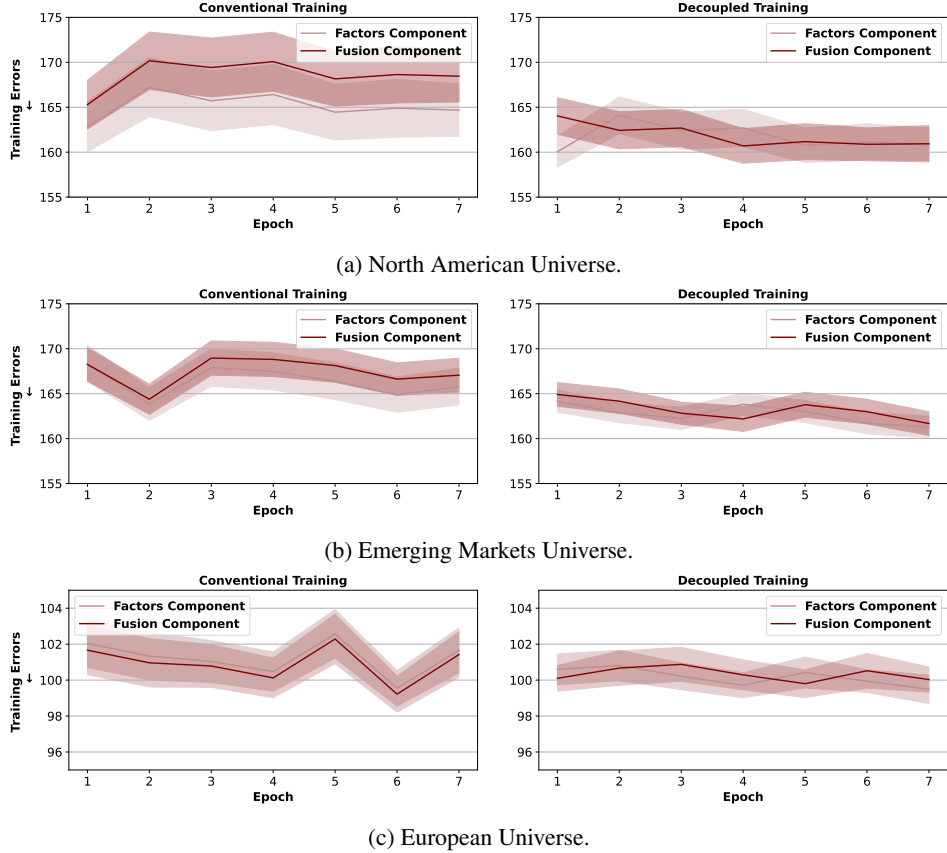


Figure 7: Training error curves of the prediction components in the mixture model under different training methods.

where  $\zeta_i$  is a vector and thus the square of its expectation is the norm  $\|\mathbb{E}[\zeta_i]\|^2$ . The third equality is obtained by applying the identity of the variance  $\text{Var}(\zeta_i) = \mathbb{E}[\|\zeta_i\|^2] - \|\mathbb{E}[\zeta_i]\|^2$  to replace  $\|\mathbb{E}[\zeta_i]\|^2$ .

In contrast, in the standalone training of the prediction component  $i$  with the squared error, e.g., training the factor prediction  $\hat{r} = g_{\theta_f}(\mathbf{x}_f)$ , the stochastic gradient  $\delta_i$  and its variance over the training data are expressed as:

$$\delta_i = -2\zeta_i = -2(r - \hat{r})\nabla_{\theta_i}g_{\theta_i}(\mathbf{x}_i) \quad (21)$$

$$\text{Var}(\delta_i) = 4 \text{Var}(\zeta_i) \quad (22)$$

□

**Discussion.** For the ease of comparison, in Eq. 20 and Eq. 22, we assume a general and approximately comparable  $\zeta_i$  across the mixture and standalone training cases. This assumption can hold when the individual prediction components do not produce drastically different predictions or when  $p(I|\cdot)$  might be close to uniform, and individual prediction components are not too specialized during early training.

However, this assumption may not hold exactly, because the residual  $r - \hat{r}$  in the standalone training is tied to the corresponding prediction component. In the mixture model, the residual depends on the predictions of all components and the probabilities.

Despite this, the proposition remains meaningful because the key result of Proposition 1 is not about the absolute value of the variance but its structural entanglement: the variances of  $\zeta_i$  and  $p_i$  are multiplicatively coupled with expectation terms in Eq. 20. This entanglement introduces additional variance into each prediction component's stochastic update, which leads to instability or convergence issues in training, as shown in Fig. 7.

Specifically, in Eq. 20, the expected squared norm  $\mathbb{E}[\|\zeta_i\|^2]$  can be large due to the number of parameters in prediction components implemented via neural networks. As a result, even moderate fluctuations in the mixture probability  $\text{Var}(p_i)$  can induce amplified variance in the parameter updates, increasing optimization noise and potentially slowing or destabilizing convergence. Additionally, since the residual  $r - \hat{r}$  of the mixture model is influenced by all prediction components, an inaccurate component can inflate the residual, thereby increasing the variance  $\text{Var}(\zeta_i)$  in Eq. 20.

## B Theoretical Insights of Decoupled Training

In this part, we discuss the implications of the decoupled training formulation and its connection to variational inference [9, 76], emphasizing its theoretical grounding and practical relevance.

In the decoupled training, we formulate the distribution matching as the KL divergence between the trainable distribution  $p_\phi(I | \mathbf{x}_f, \mathbf{x}_n)$  and the target distribution  $p_{\hat{\theta}_f, \hat{\theta}_u}(I | \mathbf{x}_f, \mathbf{x}_n, r)$  realized with the parameter estimates  $\hat{\theta}_f$  and  $\hat{\theta}_u$ , as shown in Eq. 14:

$$L(\phi; \{\mathbf{x}_f, \mathbf{x}_n, r\}, \hat{\theta}_f, \hat{\theta}_u) := \text{KL} \left[ p_\phi(I | \mathbf{x}_f, \mathbf{x}_n) \parallel p_{\hat{\theta}_f, \hat{\theta}_u}(I | \mathbf{x}_f, \mathbf{x}_n, r) \right] \quad (14)$$

KL divergence is not symmetric, and minimizing the KL divergence like Eq. 14 encourages the trainable distribution  $p_\phi(I | \mathbf{x}_f, \mathbf{x}_n)$  to concentrate on modes of the target distribution  $p_{\hat{\theta}_f, \hat{\theta}_u}(I | \mathbf{x}_f, \mathbf{x}_n, r)$ , as it penalizes the assignment of probability mass to regions where the target distribution has low density. This helps make the model robust to noisy or irrelevant inputs.

Next, we interpret the decoupled learning loss function in Eq. 12 through the lens of variational inference, where a KL divergence is used to align an approximate posterior with a true posterior distribution.

We reformulate the return prediction model from the perspective of probabilistic latent variable models as:

$$p(r | \mathbf{x}_f, \mathbf{x}_n) = \sum_{i \in \{f, u\}} p(I = i) p(r | I = i, \mathbf{x}_i) \quad (23)$$

Eq. 23 takes  $I$  as a latent random variable.  $p(r | I = i, \mathbf{x}_i)$  corresponds to the prediction component in our mixture model.  $p(I = i)$  is a prior over  $I$ .

Applying variational inference to a latent variable model such as Eq. 23 seeks to maximize the evidence lower bound (ELBO) on the log likelihood [9, 76], as shown below:

$$\log p(r | \mathbf{x}_f, \mathbf{x}_n) \quad (24)$$

$$\geq \log p(r | \mathbf{x}_f, \mathbf{x}_n) - \text{KL} \left[ q(I | \mathbf{x}_f, \mathbf{x}_n) \parallel p(I | \mathbf{x}_f, \mathbf{x}_n, r) \right] \quad (25)$$

$$= \underbrace{\sum_{i \in \{f, u\}} q(I = i | \mathbf{x}_f, \mathbf{x}_n) \log p(r | I = i, \mathbf{x}_i) - \text{KL} \left[ q(I | \mathbf{x}_f, \mathbf{x}_n) \parallel p(I) \right]}_{\text{ELBO}} \quad (26)$$

In Eq. 25, the posterior distribution  $p(I | \mathbf{x}_f, \mathbf{x}_n, r)$  reflects the relative performance of each prediction component given the true return  $r$  and  $\mathbf{x}_f$  and  $\mathbf{x}_n$ .  $q(I | \mathbf{x}_f, \mathbf{x}_n)$  is the trainable distribution for approximating the true posterior distribution  $p(I | \mathbf{x}_f, \mathbf{x}_n, r)$  of the latent variable  $I$ . At test time, the true posterior  $p(I | \mathbf{x}_f, \mathbf{x}_n, r)$  is unknown, and  $q(I | \mathbf{x}_f, \mathbf{x}_n)$  servers to infer the posterior.

In parallel, we present a lower bound of Eq. 25, which leads to our decoupled training loss under certain assumptions.

$$\log p(r | \mathbf{x}_f, \mathbf{x}_n) - \text{KL} \left[ q(I | \mathbf{x}_f, \mathbf{x}_n) \parallel p(I | \mathbf{x}_f, \mathbf{x}_n, r) \right] \quad (25)$$

$$= \log \sum_{i \in \{f, u\}} p(I = i) p(r | I = i, \mathbf{x}_i) - \text{KL} \left[ q(I | \mathbf{x}_f, \mathbf{x}_n) \parallel p(I | \mathbf{x}_f, \mathbf{x}_n, r) \right] \quad (27)$$

$$\geq \sum_{i \in \{f, u\}} p(I = i) \log p(r | I = i, \mathbf{x}_i) - \text{KL} \left[ q(I | \mathbf{x}_f, \mathbf{x}_n) \parallel p(I | \mathbf{x}_f, \mathbf{x}_n, r) \right] \quad (28)$$

The inequality in Eq. 28 holds due to the concavity of the logarithm function.

Equivalently, in practice, we typically minimize the negative log-likelihood for training the model, which corresponds to minimizing the negative of Eq. 28 as follows:

$$-\underbrace{\sum_{i \in \{f, u\}} p(I = i) \log p(r|I = i, \mathbf{x}_i)}_{\mathcal{L}(\cdot)} + \underbrace{\text{KL} [q(I|\mathbf{x}_f, \mathbf{x}_n) \| p(I|\mathbf{x}_f, \mathbf{x}_n, r)]}_{\text{KL}(\cdot)} \quad (29)$$

In the following, we show that, under certain assumptions, the two terms in Eq. 29 correspond to those in the decoupled training objective Eq. 12.

Assuming that  $p(r|I = i, \mathbf{x}_i)$  follows a Gaussian distribution with constant variance, minimizing the negative log likelihood  $-\log p(r|I = i, \mathbf{x}_i)$  reduces to minimizing the squared error between the true value and predictive mean of the distribution, i.e.,  $[r - g(x)]^2$ . Meanwhile, if the prior  $p(I = i)$  is not trainable, then

$$\arg \min_{\theta_i} \mathcal{L}(\cdot) = \arg \min_{\theta_i} -\log p_{\theta_i}(r|\mathbf{x}_i, I = i) = \arg \min_{\theta_i} [r - g_{\theta_i}(x)]^2 \quad (30)$$

Consequently, the term  $\mathcal{L}(\cdot)$  in Eq. 29 amounts to the independent training term in Eq. 12.

The trainable approximate posterior  $q(I|\mathbf{x}_f, \mathbf{x}_n)$  is equivalent to the trainable distribution  $p_{\phi}(I|\mathbf{x}_f, \mathbf{x}_n)$  used in the distribution matching term Eq. 14 of the decoupled training. The target distribute  $p_{\theta_f, \theta_u}(I|\mathbf{x}_f, \mathbf{x}_n, r)$  in Eq. 14 instantiates the posterior distribution  $p(I|\mathbf{x}_f, \mathbf{x}_n, r)$  in Eq. 29, as the posterior distribution reduces to Eq. 15 under a uniform prior of  $p(I = i)$ . Overall, the distribution matching in Eq. 14 corresponds to the  $\text{KL}(\cdot)$  term in the variational inference objective.

## C Experiment Details and Full Results

### C.1 Datasets

Table 3 presents the main categories of these factors. Our factors are grounded in financial theories and capture a range of stock characteristics. The total number of factors is  $\sim 200$ .

Table 3: Quantitative Factor Categories

Quality, Size, Volume, Growth, Momentum, Risk, Analyst Revision, Valuation, etc.

Table 4 lists the main categories of news included in our dataset. These category labels are provided directly by the data vendor alongside news data. Since our focus is on return prediction for stock selection, we primarily use news data that covers company-specific events such as earnings reports, ratings, outlooks, corporate actions, etc. Each piece of news has an attribute including the company identifier(s) the news is linked to.

Table 4: News Categories

Earnings, Guidance, Upgrades, Downgrades, Mergers and Acquisitions, Corporate Actions, Restructuring, Jobs, Ownerships, Short Interests, Buybacks, Equity Offerings, Management Changes, etc.

For associating news with stocks, we use a one-week look-back window for the EU and NA universes and a one-month window for the EM universe. The longer window for EM is due to its relatively lower news coverage. Then, for each data instance, we construct the newsflow using headlines from our news datasets, as the data, sourced from a professional financial vendor, provides structured and concise headlines [18, 46]. The full article content is noisier and introduces substantially higher training overhead, likely requiring a relevance-filtering step to retain only relevant information. Therefore, we leave the exploration of full content to future work.

The training and validation data span from 2003 to 2022, and the testing data cover the two-year period from 2023 to 2024. The volume of news data fluctuates annually, with a notable increase in recent years. Since the LLM used in this paper, DeBERTa, was developed around 2022, we selected 2023-2024 as the testing period to mitigate potential memorization bias from the LLM [53, 42, 47].

Table 5 presents the stats of training, validation, and testing data. The Range of News Items column indicates the number of news items in the newsflow associated with each data instance, and the Range of Tokens shows the number of tokens resulting from tokenizing the newsflow of each data instance. Our investment universes include all-cap stocks, and the coverage of news data is modest relative to these universes. Consequently, there exist instances with only one news term, resulting in a low token count, sometimes fewer than 10, as shown in Table 5.

Table 5: Stats of Training, Validation, and Testing Data.

Universe	# of Stocks	# of Training Instances	# of Validating Instances	# of Testing Instances	Range of News Items	Range of Tokens
North America	830	634214	10167	270345	[1, 98]	[8, 1866]
Emerging Markets	1090	213830	10183	263380	[1, 96]	[6, 1725]
Europe	370	201863	10094	113303	[1, 51]	[5, 914]

## C.2 Baselines

Universe refers to a portfolio that equally weights all stocks in the investment universe. Its performance is reported in the Long-Only Portfolio section.

Factors Alone represents a multiple dense neural network solely on quantitative factors [17]. Note that for a fair comparison, in our mixture model, the factors-based prediction component adopts the same model structure as this baseline.

News Alone utilizes only news by applying a prediction layer on the news representations generated by an LLM [30]. Specifically, it uses the encoder-only LLM, i.e., DeBERTa, consistent with the model used in our fusion learning and mixture modeling approaches. We report the performance without and with enabling the fine-tuning of DeBERTa during training.

FININ is close to the representation combination approach in our fusion learning framework, but differs in that it uses market data (e.g., factors in this paper) to weight news representations before jointly passing both through a prediction layer [66].

## C.3 Implementations

For a fair comparison, we employ the encoder-only LLM, DeBERTa [31], across our fusion learning methods, mixture models, and all LLM-based baselines. DeBERTa improves upon encoder-only language models using disentangled content and position embeddings and has demonstrated competitive performance in various financial tasks [30, 49]. In contrast, larger decoder-only LLMs such as Mistral and LLaMA may risk memorizing market information during pre-training on large and recent datasets, potentially introducing bias into downstream evaluations [47, 25].

All the methods below are implemented with the PyTorch [51] and HuggingFace Transformers libraries [71].

Fusing Learning. The representation combination method is implemented by first concatenating factor features with a bottleneck representation of newsflow, which is then passed through a dense layer for fusion, followed by a linear output layer [79, 19]. We empirically find that reducing the dimensionality of the newsflow representation, using a bottleneck dense layer, generally improves performance. This is implemented by a single dense layer that compresses the LLM-generated news representation to half of its original dimension.

For the representation summation and attentive representation methods, we use two single-layer dense networks to respectively project the factor and news representations into a unified representation space [38]. To ensure fair comparison, the dimension of this unified space is matched to the output dimension of the fusion dense layer used in the representation combination method.

In the representation summation approach, the two projected representations are summed and passed directly to a linear output layer. In the attentive representation approach, the factor and news representations are used to compute attention logits via a dense layer [50, 41]. These logits define the

weighting over the two projected representations, and the resulting weighted sum is passed to the output layer.

Note that the attentive representation method is conceptually closely related to the self-attention mechanism in Transformers [64]. The weight vector learned in the dense layer can be interpreted as a query vector in self-attention, and thus the attention weights  $a_f$  and  $a_n$  in the attentive representation method represent the relevance of factors and news representations to this query.

Mixture Modeling. For mixture modeling, the fusion component is implemented as described in the representation combination method. The factor component is realized using two dense layers with skip connections [28]. The probability logits function is implemented by a dense layer on factors and news representations.

Baselines. The Factors-alone baseline follows the same architecture as the factor component in the mixture model. The News-alone baseline uses a linear output layer on top of aggregated token-level representations, following the approach in [30].

Following [66], the FININ baseline computes the weight through the scaled dot product of two representation vectors, which respectively correspond to factors and news. These two representations are obtained by respectively passing the factor and news embeddings through two separate single-layer dense networks. Then, the weighted representation of news is added to the factors' representation and fed to the output layer.

#### C.4 Training and Evaluation Setup

For training, we use the one-month forward return as the target variable, as the subsequent backtest focuses on monthly rebalanced portfolios. We conduct the training using a batch size 32 and a learning rate  $1e - 4$  with a linear decay scheduler. For regularization, we apply a dropout rate of 0.3 to the input of prediction layers and set the weight decay to  $1e - 4$ . After training, the model is evaluated on the testing period without retraining in a rolling manner.

For fine-tuning, we applied Low-Rank Adaptation (LoRA) with rank 4 to all linear layers [32]. Other techniques, including gradient checkpointing, mixed precision training, and DeepSpeed, are used to reduce GPU memory [55]. We employ a maximum context length of 4k in experiments. All models are trained for 10 epochs on  $2 \times$  A100 GPUs.

During backtesting, the long-only portfolio is constructed by selecting the stocks whose return predictions fall in the top (9th) decile of the prediction rankings. The long-short portfolio includes stocks from both the top (9th) and bottom (0th) deciles. All stocks within each portfolio are equally weighted, and both portfolios are rebalanced on a monthly basis.

#### C.5 Metrics

For portfolio performance, we report annualized returns and Sharpe ratios over the testing period, along with charts of cumulative returns. Additionally, we present the bar charts of decile returns to provide insights into the sources of portfolio performance.

Decile Return, or the return per predicted decile, is derived in the following way [30]. At each rebalancing date, stocks are sorted by predicted returns and grouped into 10 deciles, labeled  $d = 0, \dots, 9$ . For each decile  $d$ , we calculate the average return of the stocks within that decile. These decile-level returns are then aggregated over the testing period to obtain the final decile return profile.

We also report two prediction performance metrics. Mean Absolute Percentage Error (MAPE) measures the average of the absolute percentage differences between predicted and actual values. We chose MAPE over RMSE or MSE because it expresses the error relative to the actual value, making it less sensitive to outliers and useful for comparing errors across value scales.

Information Coefficient (IC) quantifies the rank correlation between predicted and actual values [24]. It is particularly relevant for return prediction tasks, as stock selection often depends on the ranking of predicted returns. A high IC indicates strong alignment between the predicted and actual rankings, which typically leads to better portfolio performance.

## C.6 Results of the North American Universe

Table 6: Portfolio and prediction performance of the North American Universe. The best and second-best results are highlighted with dark gray █ and light gray █ boxes, respectively.

	Long-only Portfolios		Long-short Portfolios		Prediction Metrics	
	Ann. Return % (↑)	Sharpe Ratio (↑)	Ann. Return % (↑)	Sharpe Ratio (↑)	MAPE (↓)	IC (↑)
Universe	12.37	0.84	—	—	—	—
Factors Alone	22.31	0.81	22.34	1.26	1.352	0.018
News Alone	20.96	1.03	1.08	0.18	1.092	-0.0
FININ	23.12	0.83	18.16	1.16	1.467	0.019
Fusion Combination	32.43	1.0	28.41	1.64	1.402	0.031
Fusion Summation	20.42	0.76	16.13	1.03	1.465	0.017
Fusion Attention	21.73	0.73	19.59	0.87	1.302	-0.005
Mixture Conventional	23.27	0.75	29.32	1.42	1.539	0.016
Mixture Decoupled	28.21	0.92	33.77	1.78	1.319	0.027

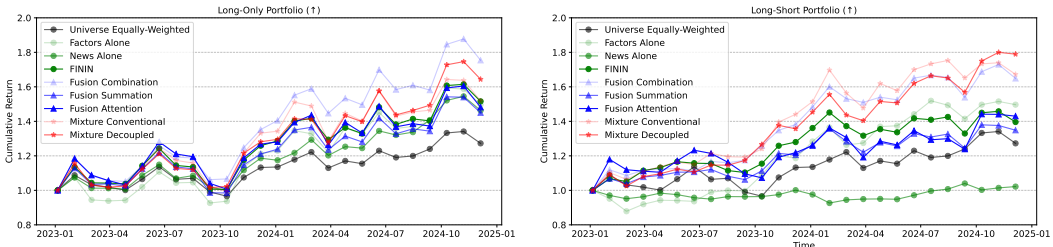


Figure 8: Portfolio Performance Charts of the North American Universe.

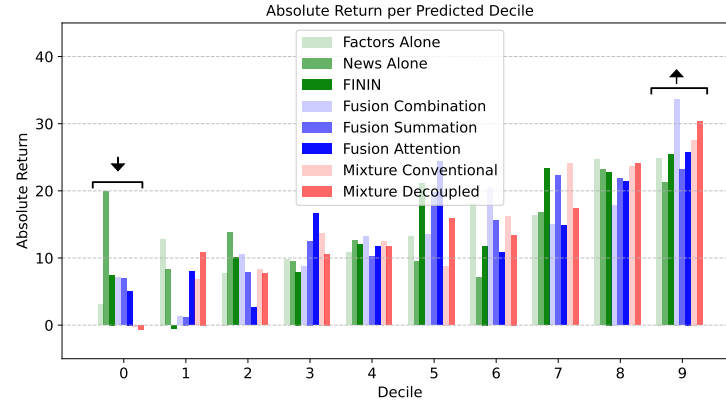


Figure 9: Decile Returns of the North American Universe. The arrows on the 0th and 9th deciles indicate the desired direction of values. A lower return is preferred for the 0th decile, as it represents the short leg of a long-short portfolio.

Table 7: Portfolio and prediction performance without and with enabling LLM fine-tuning during training for the North American Universe. The best and second-best results within each group (without fine-tuning and with fine-tuning) are highlighted with dark gray █ and light gray █ boxes.

		Long-only Portfolios		Long-short Portfolios		Prediction Metrics	
		Ann. Return % (↑)	Sharpe Ratio (↑)	Ann. Return % (↑)	Sharpe Ratio (↑)	MAPE (↓)	IC (↑)
w/o Fine-tuning	News Alone	20.96	<span style="background-color: #808080;">1.03</span>	1.08	0.18	<span style="background-color: #808080;">1.092</span>	-0.0
	FININ	23.12	0.83	18.16	1.16	1.467	0.019
	Fusion Combination	<span style="background-color: #808080;">22.43</span>	<span style="background-color: #D9D9D9;">1.0</span>	28.41	<span style="background-color: #808080;">1.64</span>	1.402	<span style="background-color: #808080;">0.031</span>
	Fusion Summation	20.42	0.76	16.13	1.03	1.465	0.017
	Fusion Attention	21.73	0.73	19.59	0.87	<span style="background-color: #808080;">1.302</span>	-0.005
	Mixture Conventional	23.27	0.75	<span style="background-color: #808080;">29.32</span>	1.42	1.539	0.016
	Mixture Decoupled	<span style="background-color: #808080;">28.21</span>	0.92	<span style="background-color: #808080;">33.77</span>	<span style="background-color: #808080;">1.78</span>	1.319	<span style="background-color: #808080;">0.027</span>
w/ Fine-tuning	News Alone	27.98	<span style="background-color: #808080;">1.33</span>	14.23	1.52	<span style="background-color: #808080;">1.118</span>	0.018
	FININ	22.09	0.81	19.65	1.24	1.468	0.02
	Fusion Combination	<span style="background-color: #808080;">28.61</span>	<span style="background-color: #D9D9D9;">0.95</span>	26.82	<span style="background-color: #808080;">1.63</span>	1.379	<span style="background-color: #808080;">0.032</span>
	Fusion Summation	20.69	0.77	18.31	1.12	1.477	0.017
	Fusion Attention	17.12	0.63	13.55	0.7	<span style="background-color: #808080;">1.298</span>	-0.004
	Mixture Conventional	26.57	0.85	<span style="background-color: #808080;">32.23</span>	1.43	1.326	0.017
	Mixture Decoupled	27.15	0.91	30.66	<span style="background-color: #808080;">1.79</span>	1.336	<span style="background-color: #808080;">0.028</span>

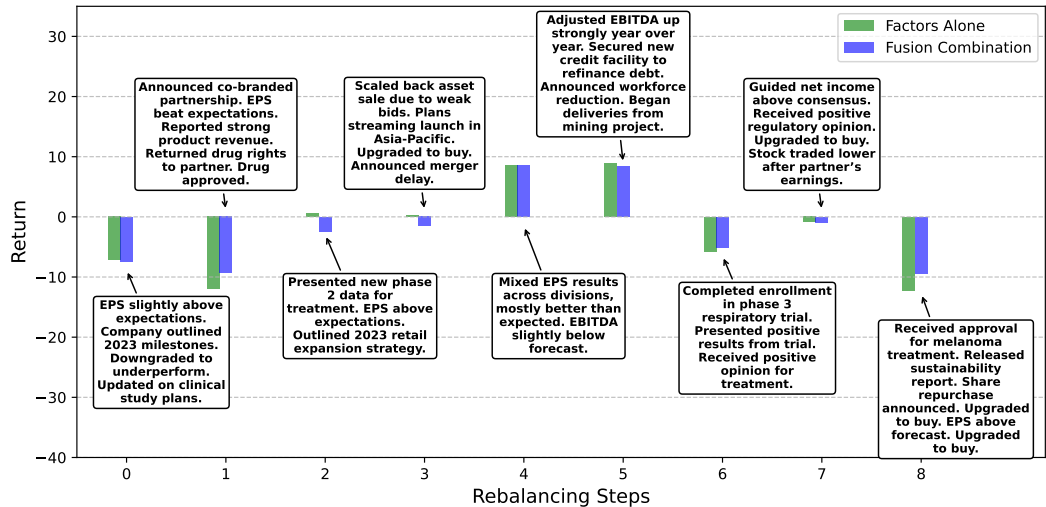


Figure 10: Qualitative Illustration of News Relevance at Rebalancing Steps in the North American Universe. At a given rebalancing step, the newsflow associated with stocks in the long-only portfolio, built based on return predictions, is collected and summarized for visualization in text boxes. The accompanying bar chart presents the forward returns of portfolios constructed using predictions from the *Factors Alone* and *Fusion Combination* methods at each rebalancing step. News contributes positively when it provides relevant and complementary information beyond what is captured by quantitative factors. Conversely, it can be detrimental when the information from the news is irrelevant or already reflected in the factors.

*Observations:* For instance, at steps 0, 2, and 3, news mostly concerns earnings, sales, and ratings, which tend to carry overlapping information with the growth, quality, and other factors. As a result, *Fusion Combination* exhibits weaker performance relative to *Factors Alone*. Conversely, at steps 1, 6, and 8, news covers diverse topics such as brand partnerships, trial completion, and so on; consequently, *Fusion Combination* performs competitively.

## C.7 Results of the Emerging Markets Universe

Table 8: Portfolio and prediction performance of the Emerging Markets Universe. The best and second-best results are highlighted with dark gray  $\blacksquare$  and light gray  $\square$  boxes, respectively.

	Long-only Portfolios		Long-short Portfolios		Prediction Metrics	
	Ann. Return % ( $\uparrow$ )	Sharpe Ratio ( $\uparrow$ )	Ann. Return % ( $\uparrow$ )	Sharpe Ratio ( $\uparrow$ )	MAPE ( $\downarrow$ )	IC ( $\uparrow$ )
Universe	2.63	0.24	—	—	—	—
Factors Alone	<b>17.14</b>	<b>0.81</b>	<b>42.17</b>	<b>2.96</b>	1.461	0.049
News Alone	-3.94	-0.2	-9.67	-1.57	<b>1.194</b>	-0.015
FININ	12.9	0.72	30.02	2.15	1.445	0.046
Fusion Combination	13.36	0.75	32.35	2.21	1.452	<b>0.06</b>
Fusion Summation	13.38	0.74	28.52	1.96	1.474	0.043
Fusion Attention	11.85	0.67	14.22	1.07	<b>1.283</b>	0.003
Mixture Conventional	7.71	0.46	22.47	1.53	1.465	0.053
Mixture Decoupled	<b>18.5</b>	<b>0.94</b>	<b>42.07</b>	<b>2.93</b>	1.395	<b>0.065</b>

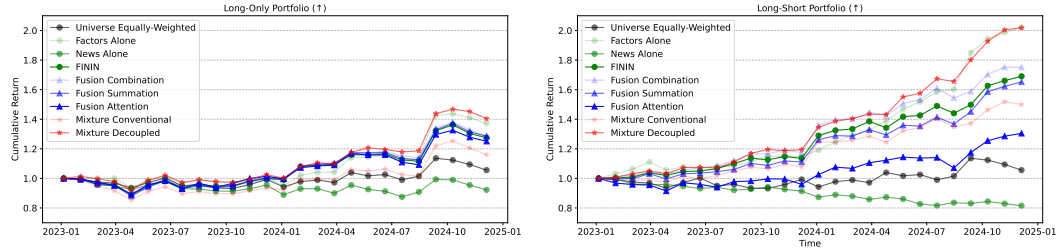


Figure 11: Portfolio Performance Charts of the Emerging Markets Universe.

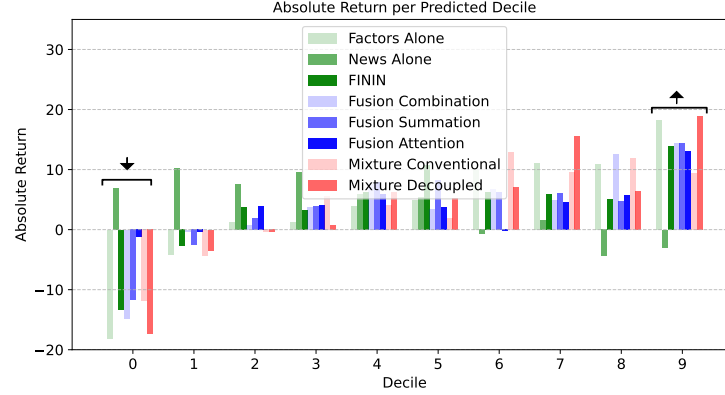


Figure 12: Decile Returns of the Emerging Markets Universe. The arrows on the 0th and 9th deciles indicate the desired direction of values. A lower return is preferred for the 0th decile, as it represents the short leg of a long-short portfolio.

Table 9: Portfolio and prediction performance without and with enabling LLM fine-tuning during training for the Emerging Markets Universe. The best and second-best results within each group (without fine-tuning and with fine-tuning) are highlighted with dark gray █ and light gray █ boxes.

		Long-only Portfolios		Long-short Portfolios		Prediction Metrics	
		Ann. Return % (↑)	Sharpe Ratio (↑)	Ann. Return % (↑)	Sharpe Ratio (↑)	MAPE (↓)	IC (↑)
w/o Fine-tuning	News Alone	-3.94	-0.2	-9.67	-1.57	<span style="background-color: #808080;">1.194</span>	-0.015
	FININ	12.9	0.72	30.02	2.15	1.445	0.046
	Fusion Combination	13.36	0.75	32.35	<span style="background-color: #D9D9D9;">2.21</span>	1.452	0.06
	Fusion Summation	<span style="background-color: #D9D9D9;">13.38</span>	0.74	28.52	1.96	1.474	0.043
	Fusion Attention	11.85	0.67	14.22	1.07	<span style="background-color: #808080;">1.283</span>	0.003
	Mixture Conventional	7.71	0.46	22.47	1.53	1.465	0.053
w/ Fine-tuning	Mixture Decoupled	<span style="background-color: #808080;">18.5</span>	<span style="background-color: #D9D9D9;">0.94</span>	<span style="background-color: #808080;">42.07</span>	<span style="background-color: #D9D9D9;">2.93</span>	1.395	<span style="background-color: #808080;">0.065</span>
	News Alone	0.38	0.1	6.43	0.87	<span style="background-color: #808080;">1.13</span>	0.02
	FININ	13.4	0.76	<span style="background-color: #D9D9D9;">31.53</span>	<span style="background-color: #D9D9D9;">2.3</span>	1.448	0.048
	Fusion Combination	12.89	0.74	30.18	2.0	1.466	<span style="background-color: #808080;">0.06</span>
	Fusion Summation	<span style="background-color: #D9D9D9;">14.87</span>	<span style="background-color: #D9D9D9;">0.81</span>	<span style="background-color: #D9D9D9;">31.53</span>	2.28	1.49	0.045
	Fusion Attention	12.36	0.7	15.45	1.22	<span style="background-color: #808080;">1.266</span>	0.003
w/ Fine-tuning	Mixture Conventional	13.03	0.73	27.18	1.84	1.484	0.049
	Mixture Decoupled	<span style="background-color: #808080;">18.18</span>	<span style="background-color: #D9D9D9;">0.93</span>	<span style="background-color: #D9D9D9;">43.49</span>	<span style="background-color: #D9D9D9;">3.03</span>	1.403	<span style="background-color: #808080;">0.065</span>

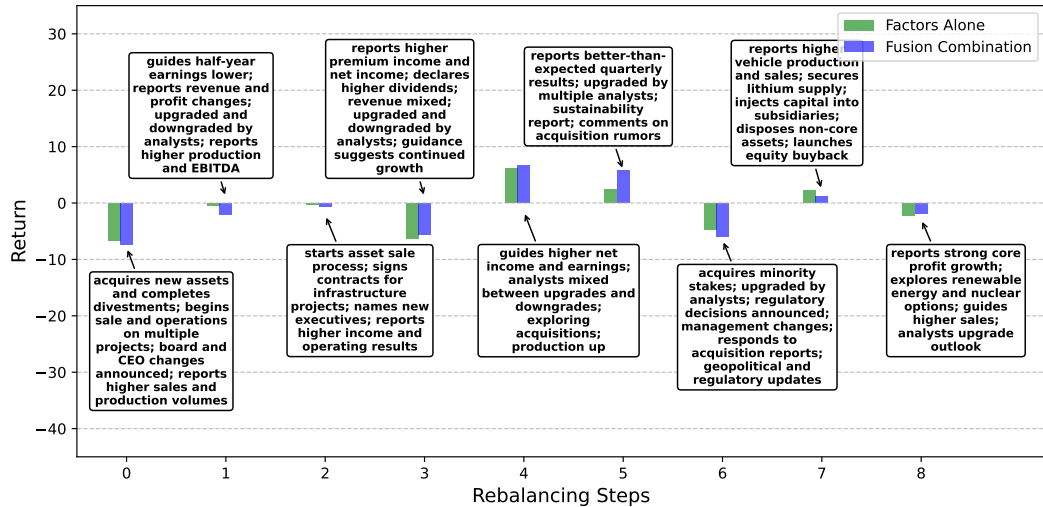


Figure 13: Qualitative Illustration of News Relevance at Rebalancing Steps in the Emerging Markets Universe. At a given rebalancing step, the newsflow associated with stocks in the long-only portfolio, built based on return predictions, is collected and summarized for visualization in text boxes. The accompanying bar chart presents the forward returns of portfolios constructed using predictions from the *Factors Alone* and *Fusion Combination* methods at each rebalancing step. News contributes positively when it provides relevant and complementary information beyond what is captured by quantitative factors. Conversely, it can be detrimental when the information from the news is irrelevant or already reflected in the factors.

*Observations:* For instance, at steps 0, 1, and 2, news predominantly concerns earnings, sales, ratings, and management changes. Such information is likely already priced in factors, causing *Fusion Combination* to struggle to distinguish redundant information from news and lag behind that of *Factors Alone*. At steps 3, 4, and 5, in addition to guidance-, income-, and ratings-related news, acquisitions and production updates also appear, appearing to provide complementary information and enhance the performance of *Fusion Combination*.

## C.8 Results of the European Universe

Table 10: Portfolio and prediction performance of the European Universe. The best and second-best results are highlighted with dark gray █ and light gray █ boxes, respectively.

	Long-only Portfolios		Long-short Portfolios		Prediction Metrics	
	Ann. Return % (↑)	Sharpe Ratio (↑)	Ann. Return % (↑)	Sharpe Ratio (↑)	MAPE (↓)	IC (↑)
Universe	6.29	0.62	—	—	—	—
Factors Alone	14.8	1.3	28.34	1.46	1.662	0.049
News Alone	9.58	0.72	1.56	0.21	1.111	0.001
FININ	17.01	1.32	24.54	1.41	1.316	0.051
Fusion Combination	19.6	1.54	32.51	1.7	1.302	0.052
Fusion Summation	16.83	1.31	25.57	1.43	1.314	0.052
Fusion Attention	14.81	1.18	20.79	1.35	1.2	0.048
Mixture Conventional	16.0	1.24	25.8	1.48	1.336	0.044
Mixture Decoupled	18.32	1.39	30.43	1.7	1.318	0.053

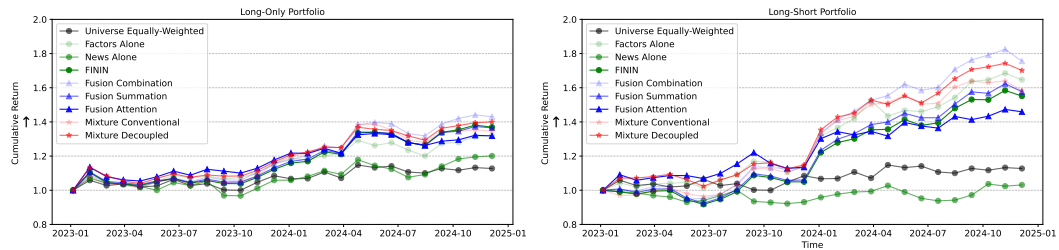


Figure 14: Portfolio Performance Charts of the European Universe.

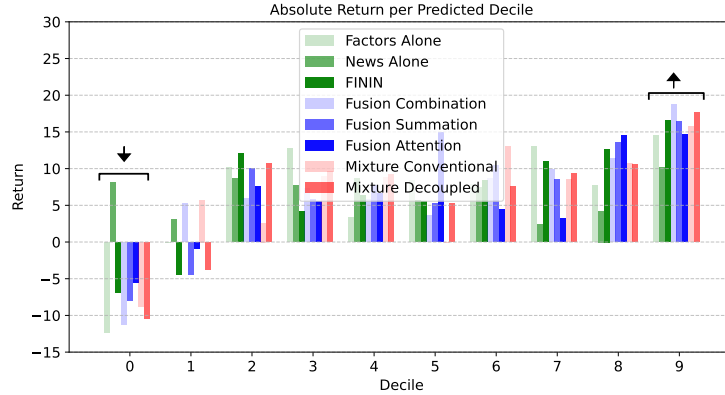


Figure 15: Decile Returns of the European Universe. The arrows on the 0th and 9th deciles indicate the desired direction of values. A lower return is preferred for the 0th decile, as it represents the short leg of a long-short portfolio.

Table 11: Portfolio and prediction performance without and with enabling LLM fine-tuning during training for the European Universe. The best and second-best results within each group (without fine-tuning and with fine-tuning) are highlighted with dark gray ■ and light gray ■ boxes.

		Long-only Portfolios		Long-short Portfolios		Prediction Metrics	
		Ann. Return % ( $\uparrow$ )	Sharpe Ratio ( $\uparrow$ )	Ann. Return % ( $\uparrow$ )	Sharpe Ratio ( $\uparrow$ )	MAPE ( $\downarrow$ )	IC ( $\uparrow$ )
w/o Fine-tuning	News Alone	9.58	0.72	1.56	0.21	<span style="background-color: #808080; border: 1px solid black; padding: 0 2px;">1.111</span>	0.001
	FININ	17.01	1.32	24.54	1.41	<span style="background-color: #D9D9D9; border: 1px solid black; padding: 0 2px;">1.316</span>	0.051
	Fusion Combination	<span style="background-color: #808080; border: 1px solid black; padding: 0 2px;">19.6</span>	<span style="background-color: #808080; border: 1px solid black; padding: 0 2px;">1.54</span>	<span style="background-color: #808080; border: 1px solid black; padding: 0 2px;">32.51</span>	<span style="background-color: #808080; border: 1px solid black; padding: 0 2px;">1.7</span>	1.302	0.052
	Fusion Summation	16.83	1.31	25.57	1.43	1.314	0.052
	Fusion Attention	14.81	1.18	20.79	1.35	<span style="background-color: #808080; border: 1px solid black; padding: 0 2px;">1.2</span>	0.048
	Mixture Conventional	16.0	1.24	25.8	1.48	1.336	0.044
	Mixture Decoupled	<span style="background-color: #808080; border: 1px solid black; padding: 0 2px;">18.32</span>	<span style="background-color: #808080; border: 1px solid black; padding: 0 2px;">1.39</span>	<span style="background-color: #808080; border: 1px solid black; padding: 0 2px;">30.43</span>	<span style="background-color: #808080; border: 1px solid black; padding: 0 2px;">1.7</span>	1.318	<span style="background-color: #808080; border: 1px solid black; padding: 0 2px;">0.053</span>
w/ Fine-tuning	News Alone	7.54	0.74	-0.03	0.03	<span style="background-color: #808080; border: 1px solid black; padding: 0 2px;">1.073</span>	-0.005
	FININ	18.77	1.45	29.4	1.62	1.317	0.049
	Fusion Combination	<span style="background-color: #808080; border: 1px solid black; padding: 0 2px;">20.15</span>	<span style="background-color: #808080; border: 1px solid black; padding: 0 2px;">1.5</span>	<span style="background-color: #808080; border: 1px solid black; padding: 0 2px;">32.27</span>	<span style="background-color: #808080; border: 1px solid black; padding: 0 2px;">1.85</span>	1.308	<span style="background-color: #808080; border: 1px solid black; padding: 0 2px;">0.053</span>
	Fusion Summation	19.78	<span style="background-color: #808080; border: 1px solid black; padding: 0 2px;">1.53</span>	30.25	1.63	1.313	0.05
	Fusion Attention	17.32	1.35	23.01	1.43	<span style="background-color: #808080; border: 1px solid black; padding: 0 2px;">1.189</span>	0.048
	Mixture Conventional	14.97	1.21	23.13	1.43	1.286	0.048
	Mixture Decoupled	18.42	1.4	31.04	<span style="background-color: #808080; border: 1px solid black; padding: 0 2px;">1.73</span>	1.323	<span style="background-color: #808080; border: 1px solid black; padding: 0 2px;">0.053</span>

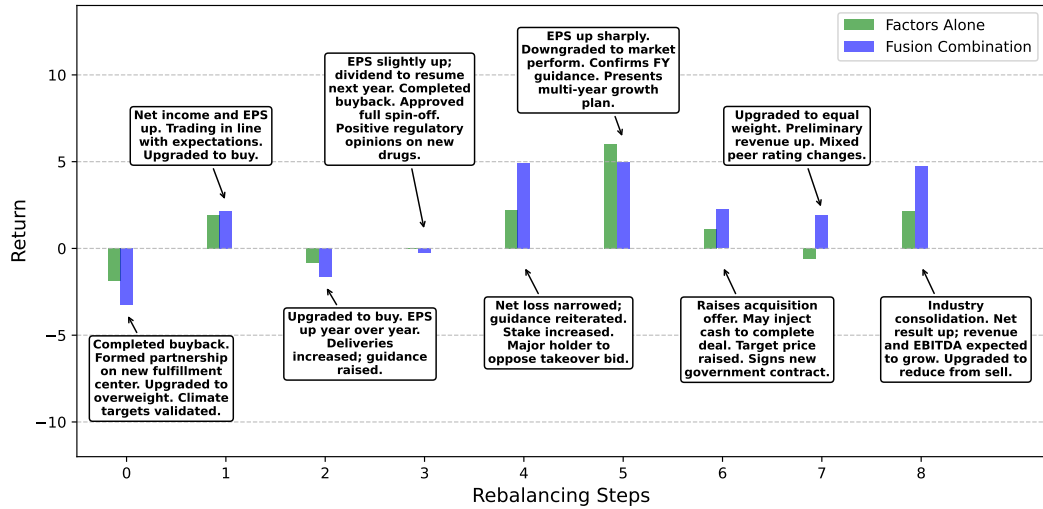


Figure 16: Qualitative Illustration of News Relevance at Rebalancing Steps in the European Universe. At a given rebalancing step, the newsflow associated with stocks in the long-only portfolio, built based on return predictions, is collected and summarized for visualization in text boxes. The accompanying bar chart presents the forward returns of portfolios constructed using predictions from the *Factors Alone* and *Fusion Combination* methods at each rebalancing step. News contributes positively when it provides relevant and complementary information beyond what is captured by quantitative factors. Conversely, it can be detrimental when the information from the news is irrelevant or already reflected in the factors.

*Observations:* For instance, at steps 0, 2, and 3, news related to earnings, buybacks, and guidance appears to bring little additional information, given the presence of growth and price-based factors in our data. In these cases, *Fusion Combination* performs worse than *Factors Alone*. In contrast, at steps 6, 7, and 8, the news additionally covers new contracts, acquisitions, industry consolidation, and so on, and provides different perspectives that *Fusion Combination* effectively leverages to improve performance.